Overview: Fusion of Radar Polarimetry and Numerical Atmospheric Modelling Towards an Improved Understanding of Cloud and Precipitation Processes

Silke Trömel[1,2], Clemens Simmer[1], Ulrich Blahak[3], Armin Blanke[1], Florian Ewald[4], Michael Frech[5], Mathias Gergely[5], Martin Hagen[4], Sabine Hörnig[6], Tijana Janjic[7], Heike Kalesse-Los[6], Stefan Kneifel[8], Christoph Knote[7,9], Jana Mendrok[3], Manuel Moser[10,4], Gregor Köcher[7], Kai Mühlbauer[1], Alexander Myagkov[11], Velibor Pejcic[1], Patric Seifert[12], Prabhakar Shrestha[1], Audrey Teisseire[12], Leonie von Terzi[8], Eleni Tetoni[4], Teresa Vogl[6], Christiane Voigt[10,4], Yuefei Zeng[7], Tobias Zinner[7], Johannes Quaas[6]

[1]Institute for Geosciences, Department of Meteorology, University of Bonn, Bonn, 53121, Germany
[2]Laboratory for Clouds and Precipitation Exploration, Geoverbund ABC/J, Bonn, 53121, Germany
[3]Deutscher Wetterdienst (DWD), Offenbach, 63067, Germany
[4]Institute for Physics of the Atmosphere, DLR, Oberpfaffenhofen, 82234, Germany
[5]Deutscher Wetterdienst (DWD), Observatorium Hohenpeißenberg, Hohenpeißenberg, 82383, Germany
[6]Institute for Meteorology, Universität Leipzig, Leipzig, 04103, Germany
[7]Meteorological Institute Munich, Ludwig-Maximilians-Universität München, 80333, Germany
[8]Institute of Geophysics and Meteorology, University of Cologne, 50969, Germany
[9]Faculty of Medicine, University of Augsburg, Augsburg, 86159 Germany
[10]Institute for Physics of the Atmosphere, University Mainz, Mainz, 55099, Germany
[11]Radiometer Physics GmbH, Meckenheim, 53340, Germany
[12]Leibniz Institute for Tropospheric Research (TROPOS), 04318 Leipzig, Germany

Correspondence to: Silke Trömel (silke.troemel@uni-bonn.de)

Abstract. Cloud and precipitation processes are still a main source of uncertainties in numerical weather prediction and climate change projections. The Priority Program "Polarimetric Radar Observations meet Atmospheric Modelling (PROM)", funded by the German Research Foundation (Deutsche Forschungsgemeinschaft, DFG), is guided by the hypothesis that many uncertainties relate to the lack of observations suitable to challenge the representation of cloud and precipitation processes in atmospheric models. Such observations can, however, nowadays be provided e.g. by the recently installed dual-polarization C-band weather radar network of the German national meteorological service in synergy with cloud radars and other instruments at German supersites and similar national networks increasingly available worldwide. While polarimetric radars potentially provide valuable in-cloud information e.g. on hydrometeor type, quantity, and microphysical cloud and precipitation processes, and atmospheric models employ increasingly complex microphysical modules, considerable knowledge gaps still exist in the interpretation of the observations and in the optimal microphysics model process formulations.

PROM is a coordinated interdisciplinary effort to intensify the use of polarimetric radar observations in data assimilation, which requires a thorough evaluation and improvement of parametrizations of moist processes in atmospheric models. As an overview article of the inter-journal special issue “Fusion of radar polarimetry and numerical atmospheric modelling towards an improved understanding of cloud and precipitation processes”, this article outlines the knowledge achieved in PROM during the past two years and gives perspectives for the next four years.

1 Introduction and Objectives of the priority program

A main source of uncertainty in the models used in numerical weather prediction (NWP) and climate change projections are the parametrizations of cloud and precipitation processes (Bauer et al., 2015). A major part of these uncertainties can be attributed to missing observations suitable to challenge the representation of cloud and precipitation processes employed in atmospheric models. A wealth of new information on precipitation microphysics and generating processes can be gained from observations from polarimetric weather radars and their synergistic analysis at different frequencies. The dual-polarization upgrade of the United States National Weather Service (NWS) S-Band Weather Surveillance Radar 1988 Doppler (WSR-88D) network was completed in 2013. Germany finished upgrading its C-band network to polarimetry in 2015 in parallel with other European countries. The synergistic exploitation of polarimetric precipitation radars together with measurements from cloud radars and other instrumentation available at supersites and research institutions enables for the first time a thorough evaluation and potential improvement of current microphysical parameterizations based on detailed multi-frequency remote-sensing observations. Data assimilation merges observations and models for state estimation as a prerequisite for prediction and can be seen as a smart interpolation between observations while exploiting the physical consistency of atmospheric models as mathematical constraints.

Considerable knowledge gaps still exist, however, both in radar polarimetry and atmospheric models, which still impede the full exploitation of the triangle between radar polarimetry, atmospheric models, and data assimilation and call for a coordinated interdisciplinary effort. The German Research Foundation (Deutsche Forschungsgemeinschaft, DFG) responded to this call and established the Priority Program “Polarimetric Radar Observations meet Atmospheric Modelling (PROM)“; its first 3-year funding period began in 2019, which will be followed by a second funding period starting in 2022. PROM exploits the synergy of polarimetric radar observations and state-of-the-art atmospheric models to better understand moist processes in the atmosphere, and to improve their representation in climate- and weather prediction models. The overarching goal is to extend our scientific understanding at the verges of the three disciplines, radar polarimetry – atmospheric models – data assimilation, for better predictions of precipitating cloud systems. To approach this goal the initiators of PROM at the Universities of Bonn and Leipzig in Germany identified the following five objectives (see also Trömel et al. 2018):

1) Exploitation of radar polarimetry for quantitative process detection in precipitating clouds and for model evaluation including a quantitative analysis of polarimetric fingerprints and microphysical retrievals,

2) Improvement of cloud and precipitation schemes in atmospheric models based on process fingerprints detectable in polarimetric observations,

3) Monitoring of the energy budget evolution due to phase changes in the cloudy, precipitating atmosphere for a better understanding of its dynamics,

4) Analyzing precipitation system by assimilation of polarimetric radar observations into atmospheric models for weather forecasting, and

5) Radar-based detection of the initiation of convection for the improvement of thunderstorm prediction.

In the first funding period, 14 projects (see https://www2.meteo.uni-bonn.de/spp2115) distributed over Germany contribute to at least one of these objectives. In most projects, a radar meteorologist works together with a modeller in order to successfully combine expert knowledge from both research fields. This overview article of the ACP/AMT/GMD inter-journal special issue entitled “Fusion of radar polarimetry and numerical atmospheric modelling towards an improved understanding of cloud and precipitation processes" outlines methodologies developed and results achieved from a selection of the projects during the past two years, and provides overall perspectives for the next four years. The paper is organized as follows: Section 2 explains prevailing challenges in the representation of clouds in atmospheric models, while Sect. 3 provides methodologies to extend our insight in the microphysics of clouds and precipitation by exploiting radar polarimetry. Section 4 addresses the fusion of numerical modelling and radar polarimetry via model evaluation either in radar observation space using observation operators or using microphysical retrievals. First conclusions for improved model parametrizations and for a better representation of model uncertainty in radar data assimilation are drawn. Section 5 provides a summary and perspectives for the following years.

2 Representation of clouds in atmospheric models

The representation of cloud and precipitation processes in atmospheric models is a central challenge for NWP and climate projections (e.g., Bauer et al., 2015; Forster et al., 2021), which also impact offline hydrological models by modulating the distribution of incoming solar radiation and precipitation and affecting the simulated hydrological processes such as evapotranspiration, runoff, and groundwater depths (e.g., Shrestha, 2021). While the primitive equations provide a solid theoretical basis for atmospheric model dynamics, the key diabatic processes that drive energetics and thus circulation, are poorly resolved. Important diabatic processes are linked to cloud and precipitation microphysics acting at scales of micrometres and turbulent processes ranging from several to hundreds of meters. While significant progress has been achieved by high-resolution modelling at the coarser end of this range (e.g., Heinze et al., 2017; Stevens et al., 2020), the intricate and complex microphysical processes still require parameterizations in any dynamic atmospheric model down to and including the scale of direct numerical simulations (e.g., Mellado et al., 2009).

A key uncertainty in weather prediction and climate modelling results from the still-rudimentary representation of moist processes and from the diabatic heating/cooling the models induce due to latent heat and their interaction with radiation. The generation and interpretation of past and future climate states additionally has to consider changes in microphysical processes due to anthropogenic aerosol acting, e.g., as cloud condensation nuclei and ice nucleating particles. For short-term weather prediction, the location and evolution of convective events with lifetimes of hours or less are particularly challenging, while relatively slow moving and frontal systems with lifetimes of days show reasonable predictability (Alifieri et al., 2012).

Atmospheric modelling in Germany has recently seen substantial advances both in terms of cloud-resolving simulations in NWP mode and in the implementation of ice and mixed-phase precipitation formation processes. Traditionally, different model systems were used for NWP and climate modelling, which were also both heavily used in academic research. Research with the ECHAM (the acronym is a combination of ECMWF (European Centre for Medium-Range Weather Forecasts) and Hamburg) model family originating from the NWP model of the ECMWF focused on long-term climate integrations at horizontal resolutions on the order of 100 km (Stevens et al., 2013), and the COSMO model operated at horizontal resolutions down to 2.8 km was used for NWP and reanalysis studies. Both model families are currently being replaced by the ICOsahedral Nonhydrostatic (ICON) modelling framework (Zängl et al., 2015) jointly developed by the Max-Planck Institute for Meteorology and the German national meteorological service (Deutscher Wetterdienst, DWD). Its climate version (the ICON general circulation model, ICON GCM) inherited its physics package from the ECHAM model, and the NWP version incorporated the one from the COSMO model. A third version largely based on the COSMO physics package was developed for higher resolutions (Dipankar et al., 2015) and employs a large-eddy turbulence scheme (ICON-LEM). The latter is able to operate on large domains (Heinze et al., 2017; Stevens et al., 2020) and includes aerosol-cloud interactions (Costa-Surós et al., 2020). In PROM primarily the three ICON model variants (ICON-LEM, ICON-NWP, and ICON-A/GCM) are used.

In most atmospheric models, cloud and precipitation microphysical processes are represented by bulk microphysical schemes that distinguish between different hydrometeor classes and include their specific masses as prognostic variables while their size distributions are parametrized (the ICON model considered here uses the scheme by Seifert and Beheng, 2006). Computationally much more demanding are so-called spectral-bin microphysics schemes (Khain et al., 2015), which evolve cloud- and precipitation particle size distributions discretized into size-interval bins. An example is the Hebrew University Cloud Model (HUCM) created by Khain et al. (2005) that treats both liquid and much more intricate (since ice may occur in various shapes and densities) ice crystal distributions. The model is employed by some of the PROM projects in addition to the liquid-only bin-microphysics model by Simmel et al. (2015) extended to the ice phase based on the scheme by Hashino and Tripoli (2007). For the simulation of the evolution of specific air volumes a Lagrangian particle model (McSnow; Brdar and Seifert, 2018) is used in PROM, that models ice and mixed-phase microphysical processes such as depositional growth, aggregation, riming, secondary ice generation, and melting closer to the real processes than bulk formulations. Microphysical processes including radiation-particle interactions obviously depend on particle shape; thus the evolution of shapes in particle models – and their signatures in radar observations – is instrumental for a full understanding and adequate representation of the microphysical processes in models. Advanced microphysical parametrizations such as spectral-bin or Lagrangian particle schemes are relevant for cloud-resolving models and exploited in PROM for the development and improvement of bulk parametrizations. Scientific questions about global climate require long model integrations and thus coarse spatial resolutions due to computing time constraints. At these resolutions (usually of order of 100 x 100 km^2 in the horizontal), fractional cloudiness needs to be considered when the grid-box mean relative humidity is below 100%, which requires parametrizations of subgrid-scale variability in relative humidity. Here, PROM builds on assumptions employed in the global ICON model (ICON GCM) to predict fractional cloudiness (e.g., Quaas, 2012).

3 Observational insights from polarimetric radar observations and challenges

DWD operates 17 state-of-the-art polarimetric Doppler C-band weather radars which provide a 3-D sampling of precipitating particles above Germany every five minutes. Together with their Doppler information, radars are the backbone for precipitation and nowcasting products for all meteorological services. Although precipitation monitoring is still the most widespread application of weather radars, their upgrade to polarimetry worldwide not only improves precipitation estimates;their observations are also increasingly exploited for the evaluation and improvement of the representation of cloud- and precipitation processes in atmospheric models (e.g., Gao et al., 2011; Jung et al., 2012; You et al., 2020; Wang et al., 2020). Additional observations from cloud radars nowadays available at so-called supersites (in Germany e.g., the Jülich Observatory for Cloud Evolution – Core Facility; JOYCE-CF; Löhnert et al. 2015; http://www.cpex-lab.de), universities, and research facilities (e.g. the Leipzig Aerosol and Cloud Remote Observations System; LACROS; Bühl et al., 2013) open opportunities to inform and improve atmospheric models. The use of shorter wavelengths of cloud radars shifts the sensitivity of the observations towards smaller particles and partly increases the magnitude of the received polarimetric signals (e.g. K_{DP} – the differential phase shift between horizontal and vertical polarization per distance called specific differential phase – scales with λ^{-1}), which allows for more detailed studies of ice and cloud microphysics. Polarimetric and multi-frequency radar observations allow for a more granular look at microphysical processes and provide a great data base for model evaluation, the improvement of microphysical parametrizations, and data assimilation, and thus have the potential to significantly improve both weather forecasts and climate predictions.

3.1 Multi-frequency and spectral polarimetry for ice and cloud microphysics

The PROM-project ***Understanding Ice Microphysical Processes by combining multi-frequency and spectral Radar polarImetry aNd super-parTicle modelling (IMPRINT)*** improves ice microphysical process understanding by using spectral multi-frequency and radar polarimetric observations in combination with Monte-Carlo Lagrangian super-particle modeling (Brdar and Seifert, 2018). id-latitude stratiform clouds, which occur frequently during winter time over JOYCE-CF, are the main focus . Radar polarimetric variables are well known to be particularly sensitive to the presence of asymmetric ice particles (e.g. Kumjian 2013). Only recently, also polarimetric cloud radars operating at Ka or W-band are routinely available (Oue et al. 2018; Myagkov et al, 2016; Bühl et al. 2016; Matrosov et al. 2012). Some polarimetric variables are wavelength dependent (K_{DP} is inversely proportional to the wavelength), which provides enhanced sensitivity to ice particle concentration at higher frequencies. Multi-frequency approaches are complementary to radar polarimetry as they are sensitive to larger ice particles. Most commonly, the dual wavelength ratio (DWR), defined as the logarithmic difference of the effective reflectivity Z_e at two frequencies, is used. When ice particles transition from Rayleigh into non-Rayleigh scattering from one wavelength to a higher one, the DWR increases, which allows to infer the characteristic size of the underlying size distribution. The use of three radar frequencies (e.g. X, Ka,W) extends the discernable size range; e.g. the DWR of the Ka-W combination saturates for very large particles (Kneifel et al. 2015; Ori et al. 2021). The information content can be further extended when also theDoppler spectral information is explored. The different fall velocities allow for the separation of different hydrometeors; the high Z_{DR} signal originating from small, slow falling ice crystals can be distinguished from the also low Z_{DR} signal of faster falling snow aggregates, which usually dominate the total Z_{DR}. Only few studies used so far spectral polarimetric observations for ice and snow microphysical studies (Luke et al,. 2021; Oue et al., 2018; Pfitzenmayer et al., 2018; Spek et al., 2008). The observations collected during the first multi-months winter campaign carried out at JOYCE-CF as part of the IMPRINT project provide for the first time the opportunity to investigate both, polarimetry and multi-frequency observations in the Doppler spectra space. An example is the analysis of the dendritic growth layer DGL illustrated in Fig. 1 for a snowfall event observed on 22nd January 2019 at JOYCE-CF. Especially in the upper half of the cloud, the Z_{DR} is enhanced while K_{DP} values are low (Fig. 1b-c). Starting at the -15°C isotherm, the Z_{DR} sharply decreases and shows an anti-correlation to the enhanced DWR (Fig. 1a) and K_{DP} values. These polarimetric signatures have been reported by previous studies (e.g., Moisseev et al., 2015 among others), and also the DWR increase below the -15°C level resembles the examples shown in Oue et al. (2018). Oue et al 2018 concluded in agreement with findings in Moisseev et al. (2015), that an increasing concentration of asymmetric aggregates are partly responsible for the enhanced values of K_{DP} because the number of small ice particles will decrease due to aggregation. The spectrally-resolved Z_{DR} (sZ_{DR}, Fig. 1e), however, reveals that high Z_{DR}-producing, slowly falling ice particles are still present down to the -5°C level. The spectrally resolved DWR (Fig. 1d) shows that the particles falling from above into the DGL are already partly aggregated. At -17°C, the spectra are much wider and a new spectral mode appears which is linked to the rapid sZ_{DR} increase (Fig. 1e). The new ice particle mode increases in Doppler velocity and sDWR until 20dB are reached. Unlike Z_{DR}, the K_{DP} (Fig. 1c and f) remains at values between 1-2°/km down to the -5°C level. A possible explanation of the bimodal spectra - increased sZ_{DR} and K_{DP} - might be secondary ice processes such as collisional fragmentation (Field et al., 2017). The few existing laboratory studies indicate that the number of fragments rapidly increases at -20°C, reaching a maximum at -17°C and decreasing again towards -10°C (Takahashi et al., 1995; Takahashi, 2014). This temperature dependence fits well to the observed radar signatures in the DGL, although the laboratory studies only considered collisions of solid ice spheres. As we can exclude strongly rimed particles in the snowfall case shown in Fig. 1, fragile dendritic structures growing on the surface of aggregates might be responsible, which precipitate into the DGL and might easily break into smaller pieces during particle collisions (Fig. 1d). Monte-Carlo Lagrangian super-particle model (Brdar and Seifert, 2018) simulations were recently extended in IMPRINT by a habit prediction scheme and a parameterization of ice collisional fragmentation following Phillips et al. (2017). The role of ice fragmentation and other ice microphysical processes is currently investigated with a radar observation operator for explaining the observed radar signatures of intense aggregation shown in Fig. 1.

The PROM-project ***Investigation of the initiation of convection and the evolution of precipitation using simulations and polarimetric radar observations at C- and Ka-band (IcePolCKa)*** combines observations of the C-band Polarization Diversity Doppler Radar (POLDIRAD) at the German Aerospace Center (DLR), Oberpfaffenhofen, with those of the Ka-band, Milimeter-wave cloud RAdar of the Munich Aerosol Cloud Scanner (miraMACS) at Ludwig-Maximilians-Universität (LMU), Munich. While IMPRINT combines triple-frequency zenith-pointing observations with spectral cloud radar polarimetry, IcePolCKa explores the life cycle of convective precipitation with spatially separated weather and cloud radars in order to quantify ice crystal properties in precipitation formation. The project focuses on ice particle growth and its role in precipitation formation within convective cells. Coordinated Range-Height-Indicator (RHI, varying elevation at constant azimuth) scans along the 23 km long cross-section between both radars allow to observe DWR (Fig. 2a) and Z_{DR} (Fig. 2b) fingerprints of individual convective cells. While the deviation from Rayleigh scattering with increasing ice crystal size at the cloud radar wavelength is used to distinguish regions dominated by aggregation from regions with depositional growth, the slanted perspective of the weather radar helps to narrow down the aspect ratio of ice crystals. Although the DWR technique to infer ice crystal size is well-established (e.g. Kneifel et al., 2015), assumptions about the unknown ice crystal shape are necessary. Here, simultaneous polarimetric measurements, like Z_{DR}, help to narrow down the average asphericity of ice crystals and reduce ambiguities in retrieving ice crystal size and ice water content. IcePolCKa develops an algorithm, which uses Z_H, Z_{DR} and DWR measurements from the two radars to retrieve IWC, the mean particle diameter D_m, and the aspect ratio of ice crystals using a least-squares fit between measurements and T-matrix scattering simulations. The model of horizontally aligned spheroids in combination with an effective medium approximation following Hogan et al (2012) is used to find the simplest ice particle model which explains the multi-wavelength polarimetric measurements. The approach allows to study the covariance of DWR and Z_{DR} while varying particle density, mean particle diameter D_m, and aspect ratio. More sophisticated models, such as DDA simulations of specific ice crystals, would require the knowledge of the aspect ratio,and make it hard to identify ice shape collections along these free variables. The multi-wavelength polarimetric measurements are also used as a benchmark for convective precipitation formation in NWP models, where cloud microphysics introduce substantial uncertainty (e.g. Morrison et al., 2020, Xue et al., 2017). In IMPRINT simulated microphysical processes in NWP models will be compared to fingerprints in radar observations: A nested WRF setup covering the overlap area of both radars is used to simulate convective events with microphysical schemes of varying complexity while the Cloud-resolving model Radar SIMulator (CR-SIM; Oue et al., 2020), produces synthetic radar observations, such as DWR (Fig. 2c) and Z_{DR} (Fig. 2d). Fig. 2 illustrates that the Predicted Particle Properties (P3) scheme (Morrison and Milbrandt, 2015) is able to produce DWR features of similar magnitude and variability compared to the observations, while a realistic ice particle asphericity is still missing. IcePolCKa compiled over 30 convective days of polarimetric measurements and simulations with 5 different schemes over a 2-year period., which is currently used to analyse how well these different microphysical schemes reproduce the polarimetric observations. A cell-tracking algorithm (TINT; Fridlind et al, 2019) facilitates the comparison on a cell object basis. Comparison of macrophysical cloud characteristics, such as echo top height or maximum cell reflectivity, show that the model simulates too few weak and small scale convective cells, independent of the microphysics scheme. In ongoing studies, the P3 scheme seems to better represent radar signatures within the ice phase, while a spectral bin scheme tends to better simulate radar signatures within rain, where all other schemes are not able to correctly reproduce observed Z_{DR} features.

The PROM-project ***A seamless column of the precipitation process from mixed-phase clouds employing data from a polarimetric C-band radar, a micro-rain radar and disdrometers (HydroColumn)*** characterizes precipitation processes inside a vertical atmospheric column by combining polarimetric Doppler weather radar observations with co-located measurements from micro-rain radars, disdrometers and in-situ measurements, and by relating these observations to the large-scale atmospheric thermodynamics derived from NWP models. To date, spectral analyses are mostly performed with cloud radars operating at shorter wavelengths (see previous paragraphs or, e.g., Shupe et al., 2004; Verlinde et al., 2013; Kalesse et al., 2016; Gehring et al., 2020; Li and Moisseev, 2020), but their implementation across the national C-band radar network offers prospects for operational area-wide applications, e.g. the identification of dominant precipitation particle growth processes such as aggregation or riming. ***HydroColumn*** uses the Doppler spectra measured at C-band during the operational DWD birdbath scan, that is used for monitoring the differential reflectivity (Frech and Hubbert, 2020), for the analysis of microphysical process information. Fig. 3 shows quasi-vertical profiles (QVPs; Trömel et al., 2014; Ryzhkov et al., 2016) of polarimetric variables and Doppler spectra from birdbath scans for a stratiform precipitation event monitored with the Hohenpeißenberg C-band research radar (47.8014N, 11.0097E) of DWD together with in-situ particle images obtained by the Falcon research aircraft from DLR during the BLUESKY campaign (Voigt et al., 2021) within the ***POLICE*** project (Sect.4.2.1). In-situ measurements have been performed with the Cloud, Aerosol and Precipitation Probe CAPS (Kleine et al., 2018) integrated in a wing station on the Falcon flying within a horizontal distance of about 20 km from the radar site and within about ±15 min of the radar measurements. The dendritic growth layer (DGL; Ryzhkov and Zrnic, 2019) centered around -15 °C is characterized by Z_{DR} maxima of ~ 1 dB and K_{DP} of ~ 0.2 ° km^{-1}, and a strong $Z_H$increase towards lower levels (Fig. 3a). Particle images collected at temperatures below about -15 °C indicate mostly small irregular ice particles with the number of larger particles increasing toward -15 °C (see levels L1 and L2 in Fig. 3c), and further down also reveal dendrites and plates (L3, L4). In general, aggregation and riming become highly effective particle growth mechanisms at temperatures around -7 °C (Libbrecht, 2005), and both processes result in a reduction of Z_{DR} (Fig. 3a). The vertically pointing Doppler measurements can be used here to gain a deeper insight into the particle growth process. In this case study, the Doppler measurements illustrated in Fig. 3b indicate typical ice-particle fall speeds increasing to about 2 m s^{-1} just above the melting layer and thus suggest a transition from predominantly aggregates to moderately rimed particles based on the relationship between Doppler velocity and riming degree found by Kneifel and Moisseev (2020). This conclusion is supported by the corresponding in-situ images showing increasing riming of polycrystals and aggregates toward the melting layer (L6). The analysis confirms the benefit of interpreting radar signatures from polarimetric weather radar observations in combination with vertically pointing Doppler radar measurements, which was previously pointed out for higher-frequency cloud research radars (Oue et al., 2018; Kumjian et al., 2020). This novel application of radar spectral analysis to vertically-pointing operational weather radar scans may provide a more detailed view into intense precipitation events, such as hailstorms, where the use of cloud radars is severely limited due to the strong attenuation at high radar frequencies.

3.2. Anthropogenic modifications of precipitation microphysics

The PROM-project ***Polarimetry Influenced by CCN aNd INP in Cyprus and Chile (PICNICC)*** seeks to improve our understanding of aerosol effects on microphysical growth processes in mixed-phase clouds. ***PICNICC*** exploits unique remote-sensing datasets from the LACROS suite (Radenz et al., 2021) extended with ground-based remote sensing instruments installed at Leipzig University, Universidad de Magallanes (Punta Arenas), and Cyprus University of Technology (Limassol). Thus, dual-frequency polarimetric radar observations from the polluted, aerosol-burden Northern and from the clean, pristine Southern hemisphere can be contrasted for microphysical process studies as already performed in the projector stratiform mixed-phase clouds to investigate inter-hemispheric contrasts in the efficiency of heterogeneous ice formation (Radenz et al., 2021). The PICNICC project challenges the hypothesis that higher ice crystal concentrations favour aggregation, which is expected to be more frequent for high aerosol loads and accordingly higher ice nucleating particle (INP) concentrations, while riming should prevail when supercooled liquid layers are sustained due to a scarcity of INP. Evaluating this hypothesis requires the distinction between aggregation and riming in mixed-phase cloud systems. Fig. 4 demonstrates for a deep mixed-phase cloud system passing the low-aerosol site in Punta Arenas (53°S, 71°W), Chile, on 30 August 2019, the capability of the LACROS suite when combined with a 94-GHz Doppler radar to distinguish between aggregates and rimed particles. The pattern of the 94-GHz radar reflectivity factor (Z_e, Fig. 4a) underlines the complex structure of the system. The height spectrogram of the vertical-pointing 94-GHz slanted linear depolarization ratio (SLDR, Fig. 4 e) from 08:30 UTC exhibits regions of changing shape signatures and multi-modality in the cloud radar Doppler spectra, where multiple hydrometeor populations coexist. The polarizability ratio ξe (Myagkov et al., 2016) (Fig. 4d) obtained from the RHI scans of SLDR and the co-cross correlation coefficient of horizontal and vertically polarized channels in the slanted basis ρ_s at 35 GHz (Fig. 4 b, c) is obtained allows to estimate a density-weighted hydrometeor shape. SLDR is more suited for shape classification compared to LDR. By slanting the polarization basis by 45°, the returned LDR signatures are much less sensitive to the canting angle distribution of the targets, especially at low elevation angles (Matrosov et al., 2001; Myagkov et al., 2016). The polarimetric RHI scans and the Doppler spectra data enable the retrieval of the vertical profile of the hydrometeors: Columnar-shaped bullet rosettes are formed between 2.5 km height and cloud top as indicated in the RHI scans by an elevation-constant SLDR (Fig. 4b) and an increase of ρ_s with decreasing elevation (Fig. 4c). ξ_e around 1.3 (Fig. 4d) is characteristic for slightly columnar crystals. The decreasing elevation-dependence of ρ_s already at around 3 km height (-15 to -20°C) suggests more random particle orientations; here the W-band SLDR spectra (Fig. 4e) show reduced values, likely due to the co-existence of dendritic ice crystals, which are formed preferably in this temperature range. The co-location of dendrites and columnar crystals can be explained by either splintering of the arms of the dendritic crystals or a mixing of locally produced dendrites with columnar crystals from higher up, or both. Below 2.5 km, ξ_e decreases toward unity, indicating the growth of isometric particles. Also the vertical-pointing W-Band SLDR slowly decreases toward the cloud base, while fall velocities increase (Fig. 4e). Both features are characteristic for riming, which is corroborated by co-located lidar observations that indicate liquid water in the cloud-base region (not shown). Doppler spectra profiles such as the one presented in Fig. 4e are also used in a new neural-network-based riming detection algorithm recently tailored by Vogl. et al. (2021) for vertical-pointing cloud radar observations. This new approach is insensitive to the mean Doppler velocity, which is - especially at Punta Arenas - strongly influenced by orographic mountain waves, because the radar reflectivity factor, skewness and the edge width of the Doppler spectrum is used instead.

The PROM-project ***Investigating the impact of Land-use and land-cover change on Aerosol-Cloud-precipitation interactions using Polarimetric Radar retrievals (ILACPR) analyzes*** polarimetric radar observations and model simulations simultaneous in order to improve our understanding of land-aerosol-cloud-precipitation interactions. The Terrestrial Systems Modelling Platform (TSMP; Shrestha et al., 2014; Gasper et al., 2014) developed under the DFG-funded Transregional Research Center TR32 (Simmer et al., 2015) is used t to simulate summertime convective storms passing the polarimetric X-band radar (BoXPol, e.g. Diederich et al., 2015a,b) located over Bonn, Germany. TSMP generally underestimates the convective area fraction, high reflectivities, and the width/magnitude of differential reflectivity (ZDR) columns indicative of updrafts, all leading to an underestimation of the frequency distribution for high precipitation values (Shrestha et al., 2021a). A decadal scale simulation over the region using the hydrological component of TMSP also shows that much of the variability in the simulated seasonal cycle of shallow groundwater could be linked to the distribution of clouds and vegetation (Shrestha, 2021), which further emphasizes the importance of model evaluation in representing clouds and precipitation. The fusion of radar observations and models with the aid of observation operators, allows for an extended interrogation of the effects of anthropogenic interventions on precipitation generating processes and the capabilities of numerical models to reproduce them. Here, findings from one simulated hailstorm observed on 5 July 2015 passing the city of Bonn, Germany are explained. Sensitivity simulations are conducted using large-scale aerosol perturbations and different land-cover types reflecting actual, reduced and enhanced human disturbances. While the differences in modelled precipitation in response to the prescribed forcing are below 5 %, the micro- and macrophysical pathways are found to differ, acting as a buffered system to the prescribed forcings (Stevens and Feingold, 2009; Seifert and Beheng, 2012). Fig. 5 shows vertical cross-sections reconstructed from volume scans measured with BoXPol together with simulated Z_H and Z_{DR} for the TSMP simulations with actual land-cover but perturbed condensation nuclei (CN) and ice nucleating particle (INP) concentrations. CN concentrations are 100 cm^{-3} for maritime and 1700 cm^{-3} for continental aerosol. Similarly, concentrations for dust, soot and organics are 162E3 m^3, 15E6 m^3 and 177E6 m^3, respectively, for default INP. For low/high INP, the concentration of soot and organics are decreased/increased by one order of magnitude. To generate the synthetic radar observations the Bonn Polarimetric Radar observation Operator, B-PRO, (Xie et al., 2021; Xie et al., 2016; Heinze et al., 2017; Shrestha et al., 2021b) is applied. B-PRO is based on the non-polarimetric version of EMVORADO (Zeng et al., 2016); its code part for computing unattenuated radar reflectivity on the original model grid (Blahak, 2016) has been expanded to unattenuated polarimetric variables based on spheroidal shape assumptions (T-matrix). Because the full polarimetric version of EMVORADO (Pol-EMVORADO, seeSection 4.1) was only released very recently, the model data in ILACPR has been processed using B-PRO. Preliminary comparisons between B-PRO and Pol-EMVORADO (not shown here) exhibit negligible differences in their results on the model grid, but Pol-EMVORADO is much more computationally efficient and takes effects of beam broadening and attenuation along the actual radar ray paths into account. The vertical cross sections are compared at different times marked by the vertical grey bars in the time series of Convective Area Fraction (CAF, Fig. 5 a), defined as the ratio of area with Z_H > 40 dBZ (at 2 km a.g.l.) to total storm area. On average BoXPol observations show a bit higher CAF compared to the simulations. The evolution is always similar in terms of an initial increase and intensification in the second part of the observation period, where the experiment with maritime aerosols and low INP (Mar-lowIn) is closest to the observations. All simulations show Z_H and Z_{DR} patterns comparable to BoXPol observations, however, the experiment with continental aerosol and default INP (Con-defIN, Fig. 5c) shows weaker $Z_{H,}$ while Mar-lowIN (Fig. 5d) shows somewhat higher Z_H values compared to BoXPol (see Fig 5a). The simulations with maritime CN produce low cloud droplet concentrations with larger mean diameters compared to the simulations with continental CN. Accompanied by a very strong updraft, this also leads to high concentrations of supercooled raindrops above the melting layer with broader spatial extent (due to a broader updraft region) compared to the simulations with continental CN and contributes to an enhanced growth of hail resulting in higher Z_H. Also, as shown in the time-series of the CAF, simulations with continental aerosol and default/high IN tend to exhibit similar behaviour in radar space, with the latter exhibiting higher CAF only at latter stages of the storm. The continental CN simulations with default and high IN differ in terms of simulated updraft speed and total hydrometeor content, being higher for the latter one. However, Cont-highIN produces smaller graupel and hail particles compared to Cont-defIN, resulting in similar Z_H.The experiment with continental aerosol and high INP concentration (Con-highIN, not shown) generates similar polarimetric moments to Con-lowIN. All experiments exhibit vertically extensive columns of (slightly) enhanced Z_{DR}, collocated with intense simulated updrafts reaching up to 13 to 14 km. Indeed, Z_{DR} columns emerged recently as proxies for updraft strength and ensuing precipitation enhancement (Weissmann et al., 2014; Simmer et al., 2014; Kumjian et al., 2014; Kuster et al., 2020), and research on their exploitation for nowcasting and data assimilation is ongoing. In Fig. 5c/d synthetic Z_{DR} columns are vertically extensive, while Z_{DR} values within the column stay below 0.3 dB. BoXPol observations show Z_{DR} columns reaching up to 6 km height only but with Z_{DR} values exceeding 1dB. While Z_{DR} values in the lower part of the columns are mostly generated by large raindrops, freezing drops and wet hail determine Z_{DR} in the upper parts of the column (Kumjian et al., 2014; Snyder et al., 2015). The diverging appearance of observed and synthetic Z_{DR} columns may point to deficiencies in the treatment of raindrops undergoing freezing and motivates further research. Too rapid freezing of drops combined with graupel generated from the frozen drops may generate enhanced but still low Z_{DR} up to high altitudes. Following Ilotoviz et al. (2018) such attributes of Z_{DR} columns are highly determined by the vertical velocity, hail size, and aerosol concentration, e.g. higher CN concentrations lead to higher columns with higher Z_{DR} values inside and also higher Z_H. In this case study and the specific time step shown, Mar-lowIN (i.e. with lower CN concentration) shows a wider and somewhat taller Z_{DR} column together with a more intense Z_H core (compare Fig. 5c/d). Further explanations require an improved representation of the Z_{DR} columns in the model.

4 Fusion of radar polarimetry and atmospheric models

Probably the most important and central tool for connecting polarimetric observations with numerical atmospheric models are observation operators, which generate virtual observations from the model state. These virtual observations can be directly compared with the real observations and signatures of microphysical processes including their temporal evolution. Thus, the accuracy of precipitation and cloud parameterizations can be indirectly evaluated and a database established for model optimization. Missing polarimetric process fingerprints (e.g. Kumjian, 2012) in the virtual observations may hint at model deficiencies, and model parameterizations can be adapted in order to increase the coherence between real and virtual observations. Moreover, sufficiently accurate and fast observation operators are mandatory for the direct assimilation of observations using ensemble methods.

However, bulk cloud microphysical parameterizations required for NWP models include assumptions on several critical parameters and processes which are not explicitly prognosed respectively resolved by the governing numerical model. An example are the inherently assumed particle size distributions and their relations to the prognostic moments (hydrometeor mass and number densities). Another challenge is the handling of hydrometeor parameters that are insufficiently or not at all constrained by the model's microphysics but are highly relevant for the calculation of virtual observations in the (radar) observation operator. For example, the melting state as well as shape, microstructure, and spatial orientation of the different hydrometeors are not prognostic (or not even implicitly assumed) in most operational bulk schemes. Therefore, suitable assumptions need to be made in observation operators in order to compute meaningful virtual observations. Moreover, bulk cloud microphysical schemes may only insufficiently approximate the natural variability, and the interactions between the few assumed hydrometeor classes and the size distribution moments are mainly tuned to get, e.g., the surface precipitation right. The current approximations in both numerical models and observation operators may hence translate into different sources of errors and biases of the simulated radar variables (e.g. Schinagl et al., 2019; Shrestha et al., 2021b). As an example, Fig. 7 shows too low polarimetric signals above the melting layer, which are partly caused by assumptions inherent in the observation operator (see Sect. 4.2.1). Such problems challenge both model evaluation and data assimilation. The central science questions are therefore the realism of the sensitivities of simulated radar variables to parameters in the observation operators and the models as well as effective approaches to the evaluation and improvement of moist processes parametrizations.

Another challenge for large-scale applications such as long-term model evaluations or operational real-time data assimilation based on large radar networks is the high computational demand and low speed of current polarimetric radar observation operators. Often, the operators apply some kind of pre-calculated lookup tables (LUT) of scattering properties and parallelization techniques for speed optimizations (e.g. Wolfensberger and Berne, 2018; Matsui et al., 2019; Oue et al., 2020). Despite that, radar simulations for a single timestep take - depending on the computer - on the order of minutes for one single plan position indicator (PPI) scan (Wolfensberger and Berne, 2018) or for a single model scene (CR-SIM; Oue et al., 2020). Matsui et al. (2019) state the LUT generation process of their POLARRIS-f operator to only take a few minutes when distributed to few thousands of processors, but do not elaborate on the required times for the actual simulation of the radar measurement. The operator B-PRO (Xie et al., 2016), which uses neither of these techniques, is much slower, as applications within SPP-PROM have demonstrated (Shresta et al., 2021b). While acceptable for research, real-time operational applications may pose much stricter time constraints. Therefore, an important technical goal is to provide an efficient, yet physically accurate and "state-of-the-art", polarimetric radar operator to the community, which reduces the simulation time for multi-elevation PPI scans of many stations to a few seconds.

4.1 Polarimetric radar observation operator development

Within the PROM-project ***Operation Hydrometeors,*** the up-to-now non-polarimetric radar observation operator EMVORADO (Zeng et al., 2016; Blahak and de Lozar, 2020; Blahak, 2016) has been extended to polarimetry (Mendrok et al., 2021).(Non-polarimetric) EMVORADO has been designed to efficiently simulate PPI volume scan measurements of entire radar networks from the prognostic model state of an NWP model for direct comparisons with the radar observations. EMVORADO is part of the executable of both the COSMO and ICON NWP models, which allows to run the operator within a NWP model run and to access the model state and radar variables in memory. The code is MPI- and OpenMP-parallelized and thus fully exploits the computational power of modern HPCs and avoids storing and re-reading extensive model state data to/from hard drives. This enables large-scale real-time applications such as operational data assimilation and extensive NWP model verifications using whole radar networks at high temporal resolution. Its modular nature allows for relatively easy interface development to other NWP models. An offline framework is also available, which accesses model states of one model time step from harddisk. EMVORADO includes detailed modular schemes to simulate beam bending, beam broadening and melting effects, and allows users to choose for each process between computationally cheap and physically accurate options. The operator has been used for the assimilation of radar reflectivity with positive impact on precipitation forecasts (Bick et al., 2016; Zeng et al., 2018, 2019, 2020). Currently, DWD uses EMVORADO to operationally assimilate 3D volumetric reflectivity and radial wind observations of its C-Band radar network. Key for this application is also the extensive use of precomputed lookup tables that relate (Mie-theory based) bulk reflectivity directly to hydrometeor densities and temperature. The effects of neglecting radar beam pattern and broadening and of hydrometeor fall speeds on data assimilation have been investigated in a joint effort together with the PROM-project ***Representing model error and observation Error uncertainty for Data assimilation of POLarimetric radar measurements (REDPOL)*** (Zeng et al., 2021a).
The polarimetry-extended EMVORADO, in the following referred to as Pol-EMVORADO, has inherited all features of EMVORADO, which in turn have been expanded where necessary to calculate and handle polarimetric variables. This includes, e.g., beam bending, beam broadening, and beam smoothing schemes, effective medium approximations allowing 1- and 2-layered hydrometeors with different water-ice-air mixing schemes and melting topologies, and alookup table approach for an efficient access to polarimetric observables such as Z_{DR}, LDR, ρ_{HV}, and K_{DP}. Optionally, attenuation effects can be

considered, specific and differential attenuation (A_H and A_{DP}, respectively) provided, and further output quantities derivable from the complex scattering amplitudes easily added. Pol-EMVORADO applies state-of-the-art scattering properties of spheroidal particles derived by one-layered (Mishchenko, 2000) and two-layered T-Matrix approaches (Ryzhkov et al., 2011). Assumptions on spheroid shape and orientation follow parametrizations introduced in Ryzhkov et al. (2011). The lookup table approach has been revised to accommodate additional parameters necessary to derive the full set of polarimetric radar output. For a given set of parameters affecting the hydrometeor scattering properties, the lookup tables are created only once, stored in files, and re-used for subsequent runs.

Using pre-existing lookup tables, the computations for virtual polarimetric volume scans of radar networks are very fast. For example, simulating the volume scans observations of all polarimetric parameters for of all 17 German radars takes afew seconds only on a Linux workstation (8 cores) and adds only about 1 s per radar output timestep to the model runtime when performed online during a run of ICON-D2 (DWD's operational convection-allowing ICON version with 2 km grid spacing) on DWD's NEC Aurora supercomputer. That is, simulating polarimetric radar data in intervals of 5 min as observed by DWD's weather radar network adds up to only a few percent total model runtime (Mendrok et al., 2021) making it possible to run Pol-EMVORADO for assimilation of high temporal resolution polarimetric radar data in an operational framework.Pol-EMVORADO has been incorporated into the official version of EMVORADO and can be run online (i.e. within a COSMO or ICON run) as well as offline (i.e. stand-alone with model fields from data files). Although designed as a PPI volume scan observation operator for a radar network, its output can also be provided on NWP model grids. An example of a Z_{DR} volume scan simulated by Pol-EMVORADO for the ***REDPOL*** project is shown in Fig. 6 (see also Sect. 4.2.3).

In summary, (Pol-)EMVORADO comprises a wide set of state-of-the-art features. While each of these features is provided also by other observation operators, (Pol-)EMVORADO is, to our knowledge, unique in combining them into an operator that allows to simulate virtual observations, including instrumental effects and in formats directly comparable to real observational scans, from within NWP model runs in a comparably accurate and very fast manner targeted at operational applications. Mendrok et al. (2021) give a comprehensive description of the features developed or updated for Pol-EMVORADO including details on their implementation and performance.

From the application of Pol-EMVORADO (or B-PRO, see Sect. 3.2) within PROM, a number of problems became evident. Modeling hydrometeors as homogeneous effective-medium particles (e.g. oblate spheroids) does not reproduce well the polarimetric signatures of low density hydrometeors like dendrites or aggregates typical for snow while keeping their microphysical properties (e.g. aspect ratio, degree of orientation) within realistic - observed or model-predicted - ranges and consistent between different radar frequencies. This deficiency has been demonstrated and explained from electromagnetic theory by Schrom et al. (2018). It is obvious in one case study (Shrestha et al., 2021b) and in Fig. 7, where Z_{DR} and K_{DP} in the snow-dominated layer between 2.5 and 5 km height almost entirely lack the typical observed features, i.e. bands of enhanced Z_{DR} and K_{DP} in the dendritic growth layer that then smoothly decrease to mostly positive, non-zero values towards the melting layer. This deficiency can also be observed with other polarimetric observation operators applying a T-matrix approach (see simulation-to-observation comparisons in Wolfensberger and Berne (2018), Matsui et al. (2019), Oue et al. (2020), where the lack of ZDR and KDP signatures is not discussed at all or exclusively explained by lack of secondary ice, though), which nevertheless currently constitutes the state-of-the-art in radar polarimetry. Orientation and shape of frozen and melting hydrometeors are very variable, both in nature and in the assumptions used in observation operators, which translates into large uncertainties in polarimetric radar signatures (e.g., Matsui et al., 2019; Shrestha et al., 2021b).

To tackle these challenges, it is planned to interface Pol-EMVORADO to scattering databases or other scattering models in order to enable more realistic cloud ice and aggregate snowflake scattering properties and allow for improvements or extensions of the polarimetry-related microphysical assumptions (shape/habit/microstructure, orientation and their distribution, e.g., Wolfensberger et al., 2018), particularly for (partly-)frozen hydrometeors. For PROM's 2nd phase, we have proposed to take this up guided with Lagrangian particle model information as well as to test the application of Pol-EMVORADO in an operational data assimilation environment.

4.2 Model evaluation and improvements using forward simulations and microphysical retrievals

4.2.1 Convection-resolving simulations with COSMO

In a joint effort, the PROM-projects ***Operation Hydrometeors*** and ***ILACPR*** evaluate simulated stratiform precipitation events in radar observation space and develop a sophisticated polarimetry-based hydrometeor classification and quantification for the evaluation of the representation of hydrometeors in numerical models. Based on a stratiform event monitored on 7 October 2014 with the Bonn polarimetric X-Band radar BoXPol, Fig. 7 illustrates the potential of using polarimetric observations for the evaluation and improvement of microphysical parametrizations. Fig. 7 a-f compare QVPs of measured and virtual Z_H, Z_{DR}, and K_{DP} with the Bonn Polarimetric Radar observation Operator B-PRO (Xie et al., 2021) to forecasts simulated with COSMO version 5.1 using its 2-moment cloud microphysics scheme (itype_gscp=2683; Seifert and Beheng, 2016). Due to a small spatial shift of the precipitation event in the simulations, the observations at 50.7305 N, 7.0717 E are compared with simulations at a close-by grid point at 51.1 N, 7.0717 E. As demonstrated in Shrestha et al. (2021b) using a similar stratiform precipitation event, COSMO tends to simulate considerable amounts of melting graupel partly reaching the surface, which results in higher synthetic Z_{DR} than observed (compare Fig. 7c/d) within and below the melting layer (ML). Above the ML, however, synthetic Z_{DR} already approaches 0 dB at around 6 km height, which indicates deficiencies in the ice-snow partitioning in COSMO as well as in the assumed snow morphology (soft spheroids) in the observation operator, both resulting in too low polarimetric signals. While the observed and simulated Z_H is comparable in terms of structure and magnitude - except a more pronounced observed ML - larger differences exist with respect to K_{DP} above the ML (Fig. 7e/f). While observations show bands of enhanced K_{DP} within the dendritic growth layer (DGL) centred around -15°C, the simulated K_{DP} is very weak indicating a lower crystal concentration and early aggregates compared to observations (e.g. Moisseev et al., 2015). Ice water content (IWC) above the ML retrieved from measured K_{DP} and differential reflectivity in linear scale Z_{dr}, i.e. IWC(K_{DP}, Z_{dr}) following Ryzhkov et al. (2018), agrees well with IWC modelled by COSMO in terms of structure, but has lower magnitudes (compare Fig. 7 g/h) in line with the lower simulated K_{DP}. Overall, Fig. 7 supports the hypothesis of a too strong graupel production in the simulations. ***Operation Hydrometeors*** also developed a robust radar-based hydrometeor classification (HMC) and mixing ratio quantification algorithm following Grazioli et al. (2015) and Besic et al. (2016, 2018) for the evaluation of the representation of hydrometeors in NWP models (standard output is the dominant hydrometeor type only). This HMC is based on clustering and has the advantage that the radar data are separated into clusters based on their polarimetric similarity (no theoretical preliminary calculation is needed), which are then identified as hydrometeor classes. Various clustering methods can be used here (e.g. Lukach et al. (2021)). The new method is relatively insensitive to uncertainties in the scattering properties of ice particles. Its application to the BoXPol observations above does not indicate graupel below the ML (Fig. 8a), while COSMO simulates a pronounced, thick graupel layer (Fig. 8b) including some melting graupel particles reaching the ground around 1:45 UTC. Applying the HMC to the virtual observations, however, does not reproduce a graupel layer of similar intensity (Fig. 8c), probably caused by a too strong Z_H and temperature influence (compare with Fig. 7) relative to the polarimetric variables in the classification scheme which needs further investigation. A persistent challenge in according routines is that clusters are always separated by the 0°C-level (e.g. Ribaud et al., 2019), i.e. hail or graupel are identified as clusters only below or above the melting layer. For the case study in Shrestha et al. (2021b) the simulated graupel was even more pronounced and sensitivity experiments were performed to guide model improvement: increasing the minimum critical particle diameter D_{crit}, which is required for self-collection of ice particles (aggregation) increased/improved the ice-snow partitioning, and a lower temperature threshold for snow and ice riming, T_{rime}, considerably reduced the graupel production.

Comparing state-of-the-art polarimetric retrievals of liquid water content (LWC), ice water content (IWC), particle number concentration N_t and mean particle diameter D_m (e.g. Ryzhkov et al., 2018; Ryzhkov and Zrnic, 2019; Bukovčić et al., 2020; Reimann et al., 2021; Trömel et al., 2019) with their simulated counterparts can also be used for evaluating NWP models and for data assimilation (Carlin et al., 2016). Fig. 7g/h, e.g., shows higher IWC(K_{DP}, Z_{dr}) than simulated by COSMO for the case study discussed earlier. For more solid conclusions about possible model errors, as well as for the use of retrieved quantities for data assimilation, the retrieval uncertainties must be estimated. The analysis of data collected in the ice regions of tropical convective clouds indicates e.g., that IWC(K_{DP}, Z_{dr}) yields a root-mean-square error of 0.49 gm^{-3} with the bias within 6% (Nguyen et al., 2017; 2019). Murphy et al. (2020) introduced the columnar vertical profile (CVP) methodology to follow the track of research aircrafts and better co-locate in-situ data to radar microphysical retrievals. Applying the methodology to two mesoscale convective systems, they found the best performance of polarimetric microphysical retrievals in regions of high ZDR and high KDP but recommend a much larger dataset to fully conclude on the accuracy of these retrievals.

The PROM-project ***POLarimetric signatures of ICE microphysical processes and their interpretation using in-situ observations and cloud modelling (POLICE)*** evaluates radar retrievals and models using in particular in-situ observations of microphysical cloud parameters from the research aircrafts HALO (e.g. Wendisch et al., 2016; Voigt et al., 2017) and Falcon (e.g. Voigt et al., 2010; Voigt et al., 2014; Flamant et al., 2017). Currently, ground-based polarimetric radar measurements and aircraft in-situ data from the Olympic Mountain Experiment OLYMPEX (Houze et al., 2017; Heymsfield et al., 2018) are exploited to investigate riming processes and to evaluate retrievals of ice water content (IWC), particle number concentration

N_t, and mean particle diameter D_m (e.g. Ryzhkov et al., 2018; Ryzhkov and Zrnic, 2019; Bukovčić et al., 2020; Carlin et al. 2021). The OLYMPEX mission took place on the Olympic Peninsula of Washington State (USA) from November 2015 through February 2016. University of North Dakota's (UND) Cessna Citation II equipped with an in-situ cloud payload overpassed the National Science Foundation (NSF) Doppler On Wheels (DOW, mobile polarimetric X-band radar with about 60 km range and 74 m radial resolution), placed in the Chehalis Valley at Lake Quinault (47.48° N, 123.86° W, 64 m altitude) performing RHI scans within an azimuthal sector of 22°. Measurements and microphysical retrievals of the DOW and the Citation, respectively, are currently evaluated and will then be compared at matched space-time coordinates for several flight transects.

4.2.2 Climate simulations with ICON-GCM

A major part of the uncertainties in representing clouds and precipitation in atmospheric models can be attributed to unresolved variability that affects resolved variables via non-linear processes. Current climate model horizontal resolutions are on the order of 100 km. But even for NWP models, which have resolutions between 10 km for global and 1 km for regional simulations, most cloud processes remain unresolved. The project ***Climate model PArametrizations informed by RAdar (PARA)*** evaluates and improves the representation of cloud and precipitation processes in particular for climate models and focuses on precipitation formation in ice clouds. Since most surface precipitation over continents and extra-tropical oceans involve the ice phase (Mülmenstädt et al., 2015; Field and Heymsfield, 2015) its reliable representation is paramount and thus the focus of ***PARA***. Microphysical parameterizations typically consider only the mean cloud liquid or ice water content to compute process rates, which causes biases in all nonlinear processes including radiation (e.g., Cahalan 1994; Carlin et al., 2002) and precipitation formation (e.g., Pincus and Klein, 2000). Realistic results thus require the tuning of process rates (e.g., Rotstayn 2000) or realistic estimates of subgrid-scale cloud variability and its inclusion in the process parametrizations. To tackle this issue, ***PARA*** exploits inherent model assumptions for treating fractional cloudiness. Since the early works of Sommeria and Deardorff (1977), atmospheric models assume or predict some notion of subgrid-scale variability of relative humidity. Some models do so by predicting cloud fraction (e.g., Tiedtke 1993), others use a diagnostic representation of the subgrid-scale probability density function (PDF) of total water specific humidity, q_t (e.g., Sundqvist et al., 1989; Smith 1990; Le Treut and Li, 1991; Rosch et al., 2015). Another option is to utilize a prognostic PDF of q_t by assuming a functional form and predicting the shape parameters of the PDF (e.g., Tompkins 2002; Neggers 2009). The German climate and weather prediction model ICON in its version dedicated to climate simulations (general circulation model version; ICON-GCM) inherits the representation of physical processes from its predecessor ECHAM6 (Stevens et al., 2013) and uses the Sundqvist et al. (1989) parameterization for a diagnostic PDF of the total-water specific humidity, q_t.

As a first step, PARA analyses the implied PDF of cloud ice using satellite observations from combined CloudSat-CALIPSO radar-lidar satellite observations (DARDAR, Delanoë et al., 2014). Interestingly, a first direct comparison of IWC profiles obtained from DARDAR with polarimetric retrievals based on the ground-based BoXPol radar shows an overall good agreement, except for columns with an integrated ice water path IWP > 1 kg m^{-2}. In these regions pronounced polarimetric signatures result in high IWC at higher altitudes, which are neither reproduced by reflectivity-only retrievals nor by the DARDAR retrievals. The statistics are currently evaluated on a larger database, which is also used to investigate the impact on the parametrizations in ICON-GCM. In the second step, a stochastic parameterisation approach is taken to allow for an unbiased computation of cloud microphysical process rates on average. Based on the cumulative distribution function (CDF), a random number generator draws from the CDF according to the simulated likelihood a plausible value of the specific ice mass based on which the microphysical process is computed. This specifically considers the formation of solid precipitation (snow) from ice clouds via aggregation and accretion processes (Lohmann and Roeckner, 1996; Stevens et al., 2013), and subsequently the evaporation of precipitation below the clouds. The result of the revised aggregation parametrizations is shown in Fig. 9. The increased aggregation rate, which is a linear function of the specific cloud ice, q_i, leads to an average decrease in q_i. The aggregation rate is directly linked to the accretion rate, which lowers the effect of q_i decrease. An investigation of the influence of the revised aggregation parametrizations on the different microphysical process rates - which are related to the ice phase - is currently performed. A detailed evaluation of the new versus old parametrizations with the ground-based polarimetric radar is on its way, and will in particular focus on the time scales of evaporation of precipitation below the cloud.

4.2.3 Data assimilation

Within an idealized framework, Jung et al. (2008, 2010) and Zhu et al. (2020) demonstrated benefits of assimilating simulated polarimetric data for the estimation of microphysical state variables. Up to now, however, direct assimilation of real polarimetric data poses great challenges due to the deficiencies of cloud and precipitation schemes in NWP models in realistically representing and providing the necessary information (optimally the distribution of particle size, shape and orientations in all model grid boxes) required by a polarimetric radar observation operator and therefore causing large representation error (Janjic et al., 2018). Both the specification of model error to examine uncertainty in microphysics (Feng et al., 2021) and the specification of the observation error for polarimetric radar observations that include estimates of the representation error (Zeng et al., 2021b), are investigated in the PROM-project ***REDPOL***. For the assimilation of radar reflectivity with an ensemble Kalman filter, several approaches for including model errors during data assimilation are explored, including 1) additive noise with samples representing large-scale uncertainty (see Zeng et al., 2018), 2) combination of large scale and unresolved scale uncertainty (Zeng et al., 2019), and finally 3) adding to these warm bubble triggering of convective storms in case they are missing in the one hour forecast but present in corresponding observations (Zeng et al., 2020). Applying Pol-EMVORADO to the analysis obtained by assimilating radar reflectivity from theGerman C-Band network), Fig. 6 illustrates the resulting differences of these three techniques in Z_{DR}-space. Obviously, synthetic Z_{DR} values depend on the strategy used to specify the model error, putting another weight to the argument that assimilation of radar reflectivity alone is not sufficient to constrain the estimation of microphysical state variables, and that polarimetric information is required in addition. First results in this direction were reported by Putnam et al. (2019), who assimilated Z_{DR} below the melting layer but reported problems in assimilation of K_{DP} data for a supercell case due to high observation errors as a result of contamination from wet hail, dust and debris and nonuniform beam filling.

.

5 Summary and Perspectives

The Priority Programme ***Polarimetric Radar Observations meet Atmospheric Modelling (PROM)*** (SPP 2115, https://www2.meteo.uni-bonn.de/spp2115/) was established in April 2017 by the Senate of the Deutsche Forschungsgemeinschaft (DFG, German Research Foundation) and is designed to run for six years. PROM is a coordinated effort to foster partnerships between cloud modelers and radar meteorologists and thus to accelerate the exploitation of polarimetric weather radars to improve the representation of cloud and precipitation processes in numerical models. The first funding phase engaged in an as-complete-as-possible exploitation and understanding of nation-wide polarimetric measurements complemented by state-of-the-art measurement devices and techniques available at supersites. Bulk polarimetric measurements available over Germany are complemented with multi-frequency observations and spectral polarimetry for detailed studies of ice and cloud microphysics. Thus, modellers now hold an unprecedented amount of three-dimensional microphysics-related observational data in their hands to improve parametrizations. Key tools for the fusion of radar polarimetry and atmospheric modelling, e.g. the Monte-Carlo Lagrangian particle model McSnow and the polarimetric observation operator Pol-EMVORADO have been developed. PROM started with detailed investigations of the representation of cloud and precipitation processes in the COSMO and ICON atmospheric models exploiting polarimetric observation operators. First improvements of the 2-moment cloud- and precipitation microphysics scheme are made and more are expected in phase 2. Also intercomparisons of microphysics schemes in radar space have been performed. Phase 1 further developed microphysical retrievals, determined their uncertainties and started their exploitation for model evaluation and radar-informed parametrizations. The developed prerequisites pave the way to finally exploit polarimetry for indirect and direct data assimilation in the upcoming second funding phase.

Some tools developed in Phase 1, however, still require refinement in Phase 2. The T-matrix calculations for electromagnetic scattering by spheroidal particles represent only a crude approximation to frozen and mixed-phase hydrometeors, especially for pristine ice particles and aggregate snowflakes at cloud radar wavelengths. It is not possible to reproduce observed polarimetric signatures of snow with the T-Matrix approach (i.e. homogeneous ice-air spheroids) and realistic microphysics (shape, orientation). Refinements include interfacing to a new discrete dipole approximation (DDA)-based scattering data base for realistic ice and snow particles for all relevant weather radar wavelengths and improvements of the melting scheme of graupel and hail.

Based on the progress made, the fusion of radar polarimetry and atmospheric modelling can be approached even more aggressively in Phase 2. While objective 1 received most attention in Phase 1, more projects will exploit the observational insights and tools developed to finally improve parameterizations and assimilate polarimetric information, i.e. more emphasis will be put on Objectives 2 and 4 in Phase 2. Direct assimilation of polarimetric variables remains challenging, because NWP models need to realistically represent and provide the necessary information required by a polarimetric radar observation operator; ideally the distribution of particle size, shape and orientation would be required in all model grid boxes. Indirect assimilation of polarimetric information (e.g. microphysical retrievals, and process signatures), however, is less demanding to the model and should be pursued in parallel. Modern Bayesian data assimilation techniques are sensitive to both model- and observation operator biases, so that further work on these issues is of great importance for a successful data assimilation.

Data availability

The data presented in this paper are available through the authors upon request. Polarimetric radar data from the operational C-band radar network is also available from the German Weather Service (DWD). Specific campaign data will be published in addition.

Author contributions

Silke Trömel had the initial idea and mainly organized and structured the joint publication. Silke Trömel, Johannes Quaas, and Clemens Simmer formed the editorial team consolidating the text. All authors contributed to specific sections of the paper and commented on the paper.

Competing interests

Johannes Quaas is editor of ACP. The authors declare to have no additional conflict of interest.

Special issue statement

This article is the overview article of the ACP/AMT/GMD inter-journal special issue "Fusion of radar polarimetry and numerical atmospheric modelling towards an improved understanding of cloud and precipitation processes". It is not associated with a conference.

Acknowledgments

We gratefully acknowledge the funding of the German Research Foundation (DFG) to initialize the special priority program on the Fusion of Radar Polarimetry and Atmospheric Modelling (SPP-2115, PROM). The work of contributing authors was carried out in the framework of the projects Operation Hydrometeors (Grants TR 1023/16-1 and BL 945/2-1), IcePolCKa (HA 3314/9-1 and ZI 1132/5-1), ILACPR (Grant SH 1326/1-1), IMPRINT (Grant KN 1112/3-1), POLICE (Grants TR 1023/13-1 and VO 1504/5-1), PARA (Grants QU 311/21-1 and TR 1023/15-1), HydroColumn (Grant FR 4119/1-1), REDPOL (Grant JA 1077/5-1), and PICNICC (Grants KA 4162/2-1 and SE 2464/1-1). ILACPR gratefully acknowledges the computing time (project HBN33) granted by the John von Neumann Institute for Computing (NIC)

and provided on the supercomputer JUWELS at Jülich Supercomputing Centre (JSC).

References

Alfieria, L., Thielen, J., and Pappenberger, J.: Ensemble hydro-meteorological simulation for flash flood early detection in southern Switzerland, J. Hydrol., 424, 143-153, doi:10.1016/j.jhydrol.2011.12.038, 2012.

Bauer, P., Thorpe, A., and Brunet, G.: The quiet revolution of numerical weather prediction, Nature 525, 47–55, doi:10.1038/nature14956, 2015.

Besic, N., Gehring, J., Praz, C., Figueras i Ventura, J., Grazioli, J., Gabella, M., Germann, U., and Berne, A.: Unraveling hydrometeor mixtures in polarimetric radar measurements, Atmos. Meas. Tech., 11, 4847–4866, doi:10.5194/amt-11-4847-2018, 2018.

Besic, N., Figueras i Ventura, J., Grazioli, J., Gabella, M., Germann, U., and Berne, A.: Hydrometeor classification through statistical clustering of polarimetric radar measurements: A semisupervised approach. Atmos. Meas. Tech., 9(9), 4425-4445, 2016

Bick, T., Simmer, C., Trömel, S., Wapler, K., Stephan, K., Blahak, U., Zeng, Y., and Potthast, R.: Assimilation of 3D-radar Reflectivities with an Ensemble Kalman Filter on the Convective Scale, Quart. J. Roy. Meteor. Soc., 142, 1490–1504, 2016.

Blahak, U.: RADAR_MIE_LM and RADAR_MIELIB - Calculation of Radar Reflectivity from Model Output, COSMO Technical Report No. 28, Consortium for Small Scale Modeling (COSMO), available online http://www.cosmo-model.org/content/model/documentation/techReports/docs/techReport28.pdf, 2016.

Blahak, U. and De Lozar, A.: EMVORADO - Efficient Modular VOlume scan RADar Operator. A User's Guide, Deutscher Wetterdienst, available online http://www.cosmo-model.org/content/model/documentation/core/emvorado_userguide.pdf, 2020.

Brdar, S. and Seifert, A.: McSnow: A Monte-Carlo Particle Model for Riming and Aggregation of Ice Particles in a Multidimensional Microphysical Phase Space, J. Adv. Model. Earth Syst., 10(1), 187–206, doi:10.1002/2017MS001167, 2018.

Bukovčić, P., Ryzhkov, A., and Zrnić, D.: Polarimetric Relations for Snow Estimation—Radar Verification, Journal of Applied Meteorology and Climatology, 59(5), 991-1009, doi:10.1175/JAMC-D-19-0140.1, 2020

Bühl, J., Seifert, P., Wandinger, U., Baars, H., Kanitz, T., Schmidt, J., Myagkov, A., Engelmann, R., Skupin, A., Heese, B., Klepel, A., Althausen, D., and Ansmann, A.: LACROS: The Leipzig Aerosol and Cloud Remote Observations System, in: SPIE Remote Sensing, edited by Comeron, A., Kassianov, E. I., Schäfer, K., Stein, K., and Gonglewski, J. D., p. 889002, Dresden, Germany, doi:10.1117/12.2030911, 2013.

Bühl, J., Seifert, P., Maygkov, A., and Ansmann, A.. Measuring ice- and liquid-water properties in mixed-phase cloud layers at the Leipzig Cloudnet station, Atmos. Chem. Phys., 16, 10609-10620, doi: 10.5194/acp-16-10609-2016, 2016

Cahalan, R. F.: Bounded cascade clouds: albedo and effective thickness, Nonlinear Proc. In Geophysics., 1, 156-167, 1994.

Carlin, B., et al.: High-cloud horizontal inhomogeneity and solar albedo bias, J. Climate, 15, 2321 – 2339, 2002.

Carlin, J. T., Ryzhkov, A. V., Snyder, J. C., and Khain, A.: Hydrometeor Mixing Ratio Retrievals for Storm-Scale Radar Data Assimilation: Utility of Current Relations and Potential Benefits of Polarimetry, Mon. Weather Rev. 144(8), 2981-3001, doi:10.1175/MWR-D-15-461 0423.1., 2016.

Carlin, J. T., Reeves, H. D., and Ryzhkov, A. V.: Polarimetric Observations and Simulations of Sublimating Snow: Implications for Nowcasting. J. Appl. Meteor. Climatol., 60(8), 1035-1054, doi:10.1175/JAMC-D-21-0038.1, 2021.

Costa-Surós, M., Sourdeval, O., Acquistapace, C., Baars, H., Carbajal Henken, C., Genz, C., Hesemann, J., Jimenez, C., König, M., Kretzschmar, J., Madenach, N., Meyer, C. I., Schrödner, R., Seifert, P., Senf, F., Brueck, M., Cioni, G., Engels, J. F., Fieg, K., Gorges, K., Heinze, R., Siligam, P. K., Burkhardt, U., Crewell, S., Hoose, C., Seifert, A., Tegen, I., and Quaas, J.: Detection and attribution of aerosol–cloud interactions in large-domain large-eddy simulations with the ICOsahedral Non-hydrostatic model, Atmos. Chem. Phys., 20, 5657–5678, doi:10.5194/acp-20-5657-2020, 2020.

Delanoë, J., Heymsfield, A. J., Protat, A., Bansemer, A., and Hogan, R. J.: Normalized particle size distribution for remote sensing application, J. Geophys. Res. Atmos., 119, 4204-4227, doi:10.1002/2013JD020700, 2014.

Diederich, M., Ryzhkov, A., Simmer, C., Zhang, P., and Trömel, S.: Use of specific attenuation for rainfall measurement at X-band radar wavelengths - Part 1: Radar calibration and partial beam blockage estimation, J. Hydrometeor., 16, 2, 487-502, doi: 10.1175/JHM-D-14-0066.1, 2015a.

Diederich, M., Ryzhkov, A., Simmer, C., Zhang, P., and Trömel, S.: Use of specific attenuation for rainfall measurement at X-band radar wavelengths - Part 2: Rainfall estimates and comparison with rain gauges, J. Hydrometeor., 16, 2, 503-516, doi: 10.1175/JHM-D-14-0067.1, 2015b.

Dipankar, A., Stevens, B., Heinze, R., Moseley, C., Zängl, G., Giorgetta, M., and Brdar, S.: Large eddy simulations using the general circulation model ICON, J. Adv. Model. Earth Sy., 7, 963–986, doi.org/10.1002/2015MS000431, 2015.

Feng, Y., T. Janjic, Y. Zeng, A.Seifert, J. Min, 2021, Representing microphysical uncertainty in convective-scale data assimilation using additive noise, J. Adv. Model. Earth Sy., 2021 (submitted).

Field, P. R. and Heymsfield, A. J.: Importance of snow to global precipitation, Geophys. Res. Lett., 42, 9512–9520, doi:10.1002/2015GL065497, 2015.

Field, P. R., Lawson, R. P., Brown, P. R. A., Lloyd, G., Westbrook, C., Moisseev, D., Miltenberger, A., Nenes, A., Blyth, A., Choularton, T., Connolly, P., Buehl, J., Crosier, J., Cui, Z., Dearden, C., DeMott, P., Flossmann, A., Heymsfield, A., Huang, Y., Kalesse, H., Kanji, Z. A., Korolev, A., Kirchgaessner, A., Lasher-Trapp, S., Leisner, T., McFarquhar, G., Phillips, V., Stith, J., and Sullivan, S.: Secondary Ice Production: Current State of the Science and Recommendations for the Future, Meteorological Monographs, 58, 7.1-7.20, doi: 10.1175/AMSMONOGRAPHS-D-16-0014.1, 2017

Forster, P., Storelvmo, T., Armour, K., Collins, W., Dufresne, J. L., Frame, D., Lunt, D. J., Mauritsen, T., Palmer, M. D., Watanabe, M., Wild, M., and Zhang, H.: The Earth's Energy Budget, Climate Feedbacks, and Climate Sensitivity. In: Climate Change 2021: The Physical Science Basis. Contribution of Working Group I to the Sixth Assessment Report of the Intergovernmental Panel on Climate Change, Cambridge University Press, in press, 2021.

Frech, M., and Hubbert, J.: Monitoring the differential reflectivity and receiver calibration of the German polarimetric weather radar network, Atmos. Meas. Tech., 13, 1051–1069, doi: 10.5194/amt-13-1051-2020, 2020.

Gao, W., Sui, C.-H., Chen Wang, T.-C. and Chang, W.-Y.: An evaluation and improvement of microphysical parameterization from a two-moment cloud microphysics scheme and the Southwest Monsoon Experiment (SoWMEX)/Terrain-influenced Monsoon Rainfall Experiment (TiMREX) observations, J. Geophys. Res. Atmos., 116, 1-13, doi:10.1029/2011JD015718, 2011.

Gasper, F., Görgen, K., Shrestha, P., Sulis, M., Rihani, J., Geimer, M., and Kollet, S.: Implementation and scaling of the fully coupled Terrestrial Systems Modeling Platform (TerrSysMP v1. 0) in a massively parallel supercomputing environment–a case study on JUQUEEN (IBM Blue Gene/Q), Geosci. Model Dev., 7(5), 2531-2543, 2014.

Gehring, J., Oertel, A., Vignon, E., Jullien, N., Besic, N., and Berne, A.: Microphysics and dynamics of snowfall associated with a warm conveyor belt over Korea, Atmos. Chem. Phys., 20, 7373–7392, doi: 10.5194/acp-20-7373-2020, 2020.

Grazioli, J., Tuia, D., and Berne, A.: Hydrometeor classification from polarimetric radar measurements: a clustering approach, Atmos. Meas. Tech., 8(1), 149-170, 2015.

Flamant, C., Knippertz, P., Fink, A.H., Akpo, A., Brooks, B., Chiu, C.J., Coe, H., Danuor, S., Evans, M., Jegede, O., Kalthoff, N., Konaré, A., Liousse, C., Lohou, F., Mari, C., Schlager, H., Schwarzenboeck, A., Adler, B., Amekudzi, L., Aryee, J., Ayoola, M., Batenburg, A.M., Bessardon, G., Borrmann, S., Brito, J., Bower, K., Burnet, F., Catoire, V., Colomb, A., Denjean, C., Fosu-Amankwah, K., Hill, P.G., Lee, J., Lothon, M., Maranan, M., Marsham, J., Meynadier, R., Ngamini, J., Rosenberg, P., Sauer, D., Smith, V., Stratmann, G., Taylor, J.W., Voigt, C., and Yoboué, V.: The Dynamics–Aerosol–Chemistry–Cloud Interactions in West Africa Field Campaign: Overview and Research Highlights, B. Am. Meteorol. Soc., 99, 83–104,doi:10.1175/BAMS-D-16-0256.1, 2018

Fridlind, A. M., van Lier-Walqui, M., Collis, S., Giangrande, S. E., Jackson, R. C., Li, X., Matsui, T., Orville, R., Picel, M. H., Rosenfeld, D., Ryzhkov, A., Weitz, R., and Zhang, P.: Use of polarimetric radar measurements to constrain simulated convective cell evolution: a pilot study with Lagrangian tracking, Atmos. Meas. Tech., 12, 2979–3000, doi:10.5194/amt-12-2979-2019, 2019.

Hashino, T., and Tripoli, G. J.: The Spectral Ice Habit Prediction System (SHIPS). Part I: Model Description and Simulation of the Vapor Deposition Process, J. Atmos. Sci., 64(7), 2210-2237, doi:10.1175/JAS3963.1, 2007.

Heinze, R., Dipankar, A., Henken, C. C., Moseley, C., Sourdeval, O., Trömel, S., Xie, X., Adamidis, P., Ament, F., Baars, H. Barthlott, C., Behrendt, A., Blahak, U. , Bley, S. , Brdar, S., Brueck, M., Crewell, S., Deneke, H., Girolamo, P. D., Evaristo, R., Fischer, J., Frank, C., Friederichs, P., Göcke, T., Gorges, K., Hande, L., Hanke, M., Hansen, A., Hege, H.-C., Hoose, C., Jahns, T., Kalthoff, N., Klocke, D., Kneifel, S., Knippertz, P., Kuhn, A., Laar, T., Macke, A., Maurer, V., Mayer, B., Meyer, C. I., Muppa, S. K., Neggers, R. A. J., Orlandi, E., Pantillon, F. , Pospichal, B., Röber, N., Scheck, L., Seifert, A., Seifert, P., Senf, F. , Siligam, P., Simmer, C., Steinke, S., Stevens, B., Wapler, K., Weniger, M., Wulfmeyer, V., Zängl, G., Zhang, D., and Quaas, J.: Large-eddy simulations over Germany using ICON: A comprehensive evaluation, Q. J. Roy. Meteor. Soc., 143, 69-100, doi:10.1002/qj.2947, 2017.

Heymsfield, A., Bansemer, A., Wood, N. B., Liu, G., Tanelli, S., Sy, O. O., Poellot, M., and Liu, C.: Toward Improving Ice Water Content and Snow-Rate Retrievals from Radars. Part II: Results from Three Wavelength Radar–Collocated In Situ Measurements and CloudSat–GPM–TRMM Radar Data, J. Appl. Meteor. Climatol., 57(2), 365-389. Retrieved Apr 6, 2021, from https://journals.ametsoc.org/view/journals/apme/57/2/jamc-d-17-0164.1.xml, 2018.

Hogan, R. J., Tian, L., Brown, P. R. A., Westbrook, C. D., Heymsfield, A. J., and Eastment, J. D.:. Radar Scattering from Ice Aggregates Using the Horizontally Aligned Oblate Spheroid Approximation, J. Appl. Meteor. Climatol., 51(3), 655-671, doi:10.1175/JAMC-D-11-074.1, 2012.

Ilotoviz, E., Khain, A., Ryzhkov, A. V., and Snyder, J. C.: Relation between Aerosols, Hail Microphysics, and ZDR Columns, J. Atmos. Sci., 75, 1755-1781, doi:10.1175/JAS-D-17-0127.1, 2018.

Janjic, T., Bormann, N., Bocquet, M., Carton, J. A., Cohn, S. E., Dance, S. L., Losa, S. N., Nichols, N. K., Potthast, R., Waller, J. A., and Weston, P.: On the representation error in data assimilation, Q. J. R. Meteorol. Soc., 144:713, 1257-1278, 2018.

Jung, Y., Xue, M., Zhang, G., and Straka, J.: Assimilation of simulated polarimetric radar data for a convective storm using ensemble Kalman filter. Part II: Impact of polarimetric data on storm analysis, Mon. Wea. Rev., 136, 2246–2260, doi:10.1175/2007MWR2288.1, 2008.

Jung, Y., Xue, M., and Zhang, G.: Simultaneous Estimation of Microphysical Parameters and the Atmospheric State Using Simulated Polarimetric Radar Data and an Ensemble Kalman Filter in the Presence of an Observation Operator Error, Mon. Wea. Rev., 138, 539–562, doi:10.1175/2009MWR2748.1, 2010.

Jung, Y., Xue, M., and Tong, M.: Ensemble Kalman Filter Analyses of the 29—30 May 2004 Oklahoma Tornadic Thunderstorm Using One- and Two-Moment Bulk Microphysics Schemes, with Verification against Polarimetric Radar Data, Mon. Wea. Rev., 140, 1457-1475, doi: MWR-D-11-00032.1, 2012

Kalesse, H., Szyrmer, W., Kneifel, S., Kollias, P., and Luke, E.: Fingerprints of a riming event on cloud radar Doppler spectra: observations and modeling, Atmos. Chem. Phys., 16, 2997–3012, doi: 10.5194/acp-16-2997-2016, 2016.

Khain, A., Rosenfeld, D., and Pokrovsky, A.: Aerosol impact on the dynamics and microphysics of convective clouds, Q. J. R. Meteorol. Soc., 131, 2639–2663, doi:10.1256/qj.04.62, 2005.

Khain, A. P., Beheng, K. D., Heymsfield, A., Korolev, A., Krichak, S. O., Levin, Z., Pinsky, M., Phillips, V., Prabhakaran, T., Teller, A., et al.: Representation of microphysical processes in cloud-resolving models: Spectral (bin) microphysics versus bulk parameterization, Rev. Geophys., 53, 247– 322, doi:10.1002/2014RG000468, 2015.

Kleine, J., Voigt, C., Sauer, D., Schlager, H., Scheibe, M., Kaufmann, S. , Jurkat-Witschas, T., Kärcher, B., and Anderson B.: In situ observations of ice particle losses in a young persistent contrail, Geophs. Res. Lett., doi:10.1029/2018GL079390, 2018.

Kneifel S., A. von Lerber, J. Tiira, D. Moisseev, P. Kollias, and J. Leinonen: Observed Relations between Snowfall Microphysics and Triple-frequency Radar Measurements, J. Geophys. Res., 120, 6034-6055, doi: 10.1002/2015JD023156, 2015.

Kneifel, S., and Moisseev, D.: Long-term statistics of riming in non-convective clouds derived from ground-based Doppler cloud radar observations, J. Atmos. Sci., 77, 3495–3508, doi: 10.1175/JAS-D-20-0007.1, 2020.

Kollias, P., Albrecht, B.A., and Marks Jr F.: Why Mie?Accurate observations of vertical air velocities and raindrops using a cloud radar. Bulletin of the American Meteorological Society, 83(10),. 1471-1484, doi: 10.1175/BAMS-83-10-1471 2002

Kumjian, M.R.: Principles and applications of dual-püolarization wheather radar. Part I: Description of the polarimetric radar variables. J. Operational Meteor., 1(19), 226-242, doi: 10.15191/nwajom.2013.0119, 2013

Kumjian, M. R.: The impact of precipitation physical processes on the polarimetric radar variables, Dissertation, University of Oklahoma, Norman Campus, https://hdl.handle.net/11244/319188, 2012

Kumjian, M. R., Khain, A. P., Benmoshe, N., Ilotoviz, E., Ryzhkov, A. V., and Phillips, V. T. J.: The anatomy and physics of Z_{DR} columns: Investigating a polarimetric radar signature with a spectral bin microphysical model, J. Appl. Meteor. Climatol., 53, 1820-1843, 2014.

Kumjian, M. R., Tobin, D. M., Oue, M., and Kollias, P.: Microphysical insights into ice pellet formation revealed by fully polarimetric Ka-band Doppler radar, J. Appl. Meteor. Climatol., 59, 1557–1580, doi: 10.1175/JAMC-D-20-0054.1, 2020.

Kuster, C. M., Schuur, T. J., Lindley, T. T., and Snyder, J. C.: Using ZDR Columns in Forecaster Conceptual Models and Warning Decision-Making, Weather and Forecasting, 35(6), 2507-2522, 2020.

Le Treut, H. and Li, Z.-X.: Sensitivity of an atmospheric general circulation model to prescribed SST changes: Feedback effects associated with the simulation of cloud optical properties, Clim. Dyn., 5, 175–187, 1991.

Li, H., and Moisseev, D.: Two layers of melting ice particles within a single radar bright band: interpretation and implications, Geophys. Res. Lett., 47, e2020GL087499, doi: 10.1029/2020GL087499, 2020.

Libbrecht, K. G.: The physics of snow crystals, Rep. Prog. Phys., 68, 855–895, doi:10.1088/0034-4885/68/4/R03, 2005.

Lohmann U. und E. Roeckner, Design and performance of a new cloud microphysics scheme developed for the ECHAM general circulation model, Clim. Dyn., 12, 557-572, 1996.

Lukach, M., Dufton, D., Crosier, J., Hampton, J.M., Bennett, L. and Neely III, R.R.. Hydrometeor classification of quasi-vertical profiles of polarimetric radar measurements using a top-down iterative hierarchical clustering method. Atmos. Meas. Tech, 14(2), pp.1075-1098, 2021

Luke E.P., Yang, F., Kollias, P., Vogelmann, A.M., Maahn, M.: New insights into ice multiplication using remote-sensing observations of slightly supercooled mixed-phase clouds in the Arctic. PNAS, 118(13), e2021387118, doi:10.1073/pnas.2021387118, 2021

Matrosov, S. Y., Reinking, R. F., Kropfli, R. A., Martner, B. E., and Bartram, B. W. (2001), On the use of radar depolarization ratios for estimating shapes of ice hydrometeors in winter clouds, Journal of Applied Meteorology, 40, 479-490, doi:10.1175/1520-0450(2001)040h0479:OTUORDi2.0.CO;2.

Matsui, T., Dolan, B., Rutledge, S. A., Tao, W.-K., Iguchi, T., Barnum, J., and Lang, S. E.: POLARRIS: A POLArimetric Radar Retrieval and Instrument Simulator, J. Geophys. Res.-Atmos., 124, 4634–4657, doi:10.1029/2018JD028317, 2019.

Mellado, J.P., Stevens, B., Schmidt, H., and Peters, N.: Buoyancy reversal in cloud-top mixing layers, Q.J.R. Meteorol. Soc., 135: 963-978., doi:10.1002/qj.417, 2009.

Mendrok, J., Blahak, U., Snyder, J. C., and Carlin, J. T.: The polarimetric efficient modular volume scan radar forward operator Pol-EMVORADO, Geosci. Model Dev., 2021 (in preparation for this Special Issue).

Mishchenko, M. I.: Calculation of the amplitude matrix for a nonspherical particle in a fixed orientation, Appl. Opt. 39, 1026-1031, 2000.

Moisseev, D. N., Lautaportti, S., Tyynela, J., and Lim, S.: Dualpolarization radar signatures in snowstorms: Role of snowflake aggregation, J. Geophys. Res. Atmos., 120, 12 644–12 655, doi:10.1002/2015JD023884, 2015.

Morrison, H. and Milbrandt, J. A.: Parameterization of Cloud Microphysics Based on the Prediction of Bulk Ice Particle Properties. Part I: Scheme Description and Idealized Tests, J. Atmos. Sci., 72(1), 287-311, 2015.

Morrison, H., van Lier-Walqui, M., Fridlind, A. M., Grabowski, W. W., Harrington, J. Y., and Hoose, C., et al.: Confronting the challenge of modeling cloud and precipitation microphysics. Journal of Advances in Modeling Earth Systems, 12, e2019MS001689. doi:10.1029/2019MS001689, 2020.

Mülmenstädt, J., Sourdeval, O., Delanoë, J., and Quaas, J.: Frequency of occurrence of rain from liquid-, mixed- and ice-phase clouds derived from A-Train satellite retrievals, Geophys. Res. Lett., 42, 6502-6509, doi:10.1002/2015GL064604, 2015.

Murphy, A. M., Ryzhkov, A., & Zhang, P.: Columnar vertical profile (CVP) methodology for validating polarimetric radar retrievals in ice using in situ aircraft measurements. J. Atmos. Oceanic Technol., 37(9), 1623-1642, doi:10.1175/JTECH-D-20-0011.1, 2020.

Myagkov, A., Seifert, P., Bauer-Pfundstein, M., and Wandinger, U.: Cloud radar with hybrid mode towards estimation of shape and orientation of ice crystals, Atmos. Meas. Tech., 9, 469–489, doi:10.5194/amt-9-469-2016, 2016.

Neggers, R. A.: A dual mass flux framework for boundary layer convection. Part II: Clouds, J. Atmos. Sci., 66, 1489–1506, doi:10.1175/2008JAS2636.1, 2009.

Neto, J. D., Kneifel, S., Ori, D., Trömel, S., Handwerker, J., Bohn, B., Hermes, N., Mühlbauer, K., Lenefer, M., and Simmer, C.: The TRIple-frequency and Polarimetric radar Experiment for improving process observation of winter precipitation. Earth Syst. Sci. Data, 11, 845–863, doi: 10.5194/essd-11-845-2019, 2019.

Nguyen, C., Wolde, M., Baibakov, K., and Korolev, A.: Detection and estimation of high ice water content using X- and W-band dual-polarization airborne radar data, 38th Conf. on Radar Meteorology, Chicago, IL, Amer. Meteor. Soc., 89, https://ams.confex.com/ams/38RADAR/webprogram/Paper321101.html, 2017.

Nguyen, C. M., Wolde, M., and Korolev, A.: Determination of ice water content (IWC) in tropical convective clouds from X-band dual-polarization airborne radar, Atmos. Meas. Tech., 12, 5897–5911, doi: 10.5194/amt-12-5897-2019, 2019.

Ori, D., V. Schemann, M. Karrer, J. Dias Neto, L. von Terzi, A. Seifert, and S. Kneifel: Evaluation of ice particle growth in ICON using statistics of multi-frequency Doppler cloud radar observations, Q. J. Roy. Meteor. Soc., 146: 3830– 3849. doi:10.1002/qj.3875, 2020

Oue, M., A. Tatarevic, P. Kollias, D. Wang, K. Yu, and A.M. Vogelmann: The Cloud-resolving model Radar SIMulator (CR-SIM) Version 3.3: description and applications of a~virtual observatory, Geoscientific Model Development, 13: 1975-1998. doi: 10.5194/gmd-13-1975-2020, 2020.

Oue, M., Kollias, P., Ryzhkov, A., and Luke, E. P.: Toward exploring the synergy between cloud radar polarimetry and Doppler spectral analysis in deep cold precipitating systems in the Arctic, J. Geophys. Res. Atmos., 123, 2797–2815, doi: 10.1002/2017JD027717, 2018.

Phillips, V. T. J., Yano, J., & Khain, A. (2017). Ice Multiplication by Breakup in Ice–Ice Collisions. Part I: Theoretical Formulation, J. Atmos. Sci., *74*(6), 1705-1719

Pfitzenmayer L., Unal, C. M. H., Dufournet, Y., Ruschenberg, H. W. J.: Observing ice particle growth along fall streaks in mixed-phase clouds using spectral polarimetric radar data, Atmos. Chem. Phys., 18, 7843-7863, doi: 10.5194/acp-18-7843-2018, 2018.

Pincus, R. and Klein, S.: Unresolved spatial variability and microphysical process rates in large-scale models, J. Geophys. Res., 105, 27059 - 27065, 2000.

Putnam, B., Xue, M., Jung, Y., Snook, N., and Zhang, G.: Ensemble Kalman Filter Assimilation of Polarimetric Radar Observations for the 20 May 2013 Oklahoma Tornadic Supercell Case, Mon. Wea. Rev., 147, 2511–2533, doi:10.1175/MWR-D-18-0251.1, 2019.

Radenz, M., Bühl, J., Seifert, P., Baars, H., Engelmann, R., Barja González, B., Mamouri, R.-E., Zamorano, F., and Ansmann, A.: Hemispheric contrasts in ice formation in stratiform mixed-phase clouds: Disentangling the role of aerosol and dynamics with ground-based remote sensing, Atmos. Chem. Phys. Discuss. [preprint], https://doi.org/10.5194/acp-2021-360, in review, 2021.

Reimann, L., Simmer, C., and Trömel, S.: Dual-polarimetric radar estimators of liquid water content over Germany, Accepted for Meteorol. Z. (Contrib. Atm. Sci.), doi:10.1127/metz/2021/1072, 2021.

Ribaud, J.-F., L. A. T. Machado, and T. Biscaro: X-band dual-polarization radar-based hydrometeor classification for Brazilian tropical precipitation systems, Atmos. Meas. Tech., 12, 811–837, doi.org/10.5194/amt-12-811-2019, 2019.

Rosch, J., et al.: Analysis of diagnostic climate model cloud parameterisations using large-eddy simulations, Q. J. R. Meteorol. Soc., 141, 2199-2205, doi:10.1002/qj.2515, 2015.

Rotstayn, L. D.: On the tuning of autoconversion parameterizations in climate models, J. Geophys. Res., 105, 15,495–15,507, 2000.

Ryzhkov, A. V., Zrnic, D. S., and Gordon, B. A.: Polarimetric Method for Ice Water Content Determination, J. Appl. Meteor. Climatol., 37, 125-134, 1998.

Ryzhkov, A., Pinsky, M., Pokrovsky, A., and Khain, A.: Polarimetric Radar Observation Operator for a Cloud Model with Spectral Microphysics, J. Appl. Meteor. Climatol., 50, 873-894, 2011.

Ryzhkov, A., Zhang, P., Reeves, H., Kumjian, M., Tschallener, T., Trömel, S., and Simmer, C.: Quasi-vertical profiles – a new way to look at polarimetric radar data, J. Atmos. Oceanic Technol., 33, 551-562, doi: 10.1175/JTECH-D-15-0020.1, 2016.

Ryzhkov, A., Bukovcic, P., Murphy, A., Zhang, P., and McFarquhar, G.: Ice Microphysical Retrievals Using Polarimetric Radar Data. In Proceedings of the 10th European Conference on Radar in Meteorology and Hydrology, Ede, The Netherlands, 1–6 July 2018.

Ryzhkov, A. and Zrnic, D.: Radar Polarimetry for Weather Observations, Springer Atmospheric Sciences, 486 pp., 2019.

Schinagl, K., Friederichs, P., Trömel, S., and Simmer, C.: Gamma Drop Size Distribution Assumptions in Bulk Model Parameterizations and Radar Polarimetry and Their Impact on Polarimetric Radar Moments, J. Appl. Meteor. Climatol., 58, 467–478, doi: 10.1175/JAMC-D-18-0178.1, 2019.

Schrom, R. S. and Kumjian, M. R.: Bulk-Density Representations of Branched Planar Ice Crystals: Errors in the Polarimetric Radar Variables, J. Appl. Meteor. Climatol., 57(2), 333-346, 2018.

Seifert, A. and Beheng, K. D.: A two-moment cloud microphysics parameterization for mixed-phase clouds. Part 1: Model description, Meteorol. Atmos. Phys., 92, 45-66, doi: 10.1007/s00703-005-0112-4, 2006.

Shrestha, P., Sulis, M., Masbou, M., Kollet, S. and Simmer, C: A scale-consistent Terrestrial System Modeling Platform based on COSMO, CLM and ParFlow, Mon. Wea. Rev., 142, 3466-3483, doi: 10.1175/MWR-D-14-00029.1, 2014

Shrestha, P.: Clouds and vegetation modulate shallow groundwater table depth, 22, 753 – 763, doi:10.1175/JHM-D-20-0171.1, 2021

Shrestha, P., Trömel, S., Evaristo, R., and Simmer, C.: Evaluation of modeled summertime convective storms using polarimetric radar observations, Atmos. Chem. Phys. Discuss. [preprint], https://doi.org/10.5194/acp-2021-404, in review, 2021a.

Shrestha, P., Mendrok, J., Pejcic, V., Trömel, S., and Blahak, U.: The impact of uncertainties in model microphysics, retrievals and forward operators on model evaluations in polarimetric radar space, Geosci. Model Dev., 2021b (submitted).

Shupe, M. D., Kollias, P., Matrosov, S. Y., and Schneider, T. L.: Deriving mixed-phase cloud properties from Doppler radar spectra, J. Atmos. Oceanic Technol., 21, 660–670, doi: 10.1175/1520-0426(2004)021<0660:DMCPFD>2.0.CO;2, 2004.

Simmel, M., Bühl, J., Ansmann, A., and Tegen, I.: Ice phase in altocumulus clouds over Leipzig: remote sensing observations and detailed modeling, Atmos. Chem. Phys., 15, 10453–10470, doi:10.5194/acp-15-10453-2015, 2015.

Simmer, C., Thiele-Eich, I., Masbou, M., Amelung, W., Crewell, S., Diekkrueger, B., Ewert, F., Hendricks Franssen, H.-J., Huisman, A. J., Kemna, A., Klitzsch, N., Kollet, S., Langensiepen, M., Löhnert, U., Rahman, M., Rascher, U., Schneider, K., Schween, J., Shao, Y., Shrestha, P., Stiebler, M., Sulis, M., Vanderborght, J., Vereecken, H., van der Kruk, J., Zerenner, T., and Waldhoff, G.: Monitoring and Modeling the Terrestrial System from Pores to Catchments - the Transregional Collaborative Research Center on Patterns in the Soil-Vegetation-Atmosphere System, B. Am. Meteorol. Soc., 96, 1765–1787, doi: 10.1175/BAMS-D-13-00134.1, 2015.

Simmer, C., Adrian, G., Jones, S., Wirth, V., Goeber, M., Hohenegger, C., Janjic, T., Keller, J., Ohlwein, C., Seifert, A., Trömel, S., Ulbrich, T., Wapler, K., Weissmann, M., Keller, J., Masbou, M., Meilinger, S., Riss, N., Schomburg, A., Vormann, A., and Weingaertner, C.: HErZ - The German Hans-Ertel Centre for Weather Research. B. Am. Meteorol. Soc., 1057-1068, doi: 10.1175/BAMS-D-13-00227.1, 2014

Smith, R. N.: A scheme for predicting layer clouds and their water content in a general circulation model, Q. J. R. Meteorol. Soc., 116, 435–460, doi:10.1002/qj.49711649210, 1990.

Snyder, J.C., Ryzhkov, A.V., Kumjian, M.R., Khain, A.P., and Picca, J.C.: A ZDR column detection algorithm to examine convective storm updrafts, Weather and Forecasting, 30, 1819-1844**,** 2015.

Sommeria, G. and Deardorff, J. W.: Subgrid-scale condensation models of non-precipitating clouds, J. Atmos. Sci., 34, 344-355, 1977.

Sourdeval, O., Gryspeerdt, E., Krämer, M., Goren, T., Delanoë, J., Afchine, A., Hemmer, F., and Quaas, J.: Ice crystal number concentration estimates from lidar–radar satellite remote sensing – Part 1: Method and evaluation, Atmos. Chem. Phys., 18, 14327–14350, doi: 10.5194/acp-18-14327-2018, 2018.

Spek, A. L. J., Unal, C. M. H., Moisseev, C. N., Russchenberg, H. W. J., Chandrasekar, V., Dufournet, Y.: A New Techniques to Categorize and Retrieve the Microphysical Properties of Ice Particles above the Melting Layer Using Radar Dual-Polarization Spectral Analysis, Jtech,doi: 10.1175/2007JTECHA944.1, 2008.

Stevens, B., Acquistapace, C., Hansen, A., Heinze, R., Klinger, C., Klocke, D., Schubotz, W., Windmiller, J., Adamidis, P., Arka, I., Barlakas, V., Biercamp, J., Brueck, M., Brune, S., Buehler, S., Burkhardt, U., Cioni, G., Costa-Surós, M., Crewell, S., Crueger, T., Deneke, H., Friederichs, P., Carbajal Henken, C., Hohenegger, C., Jacob, M., Jakub, F., Kalthoff, N., Köhler, M., Van Laar, T. W., Li, P., Löhnert, U., Macke, A., Madenach, N., Mayer, B., Nam, C., Naumann, A. K., Peters, K., Poll, S. , Quaas, J., Röber, N., Rochetin, N., Rybka, H., Scheck, L., Schemann, V., Schnitt, S., Seifert, A., Senf, F., Shapkalijevski, M., Simmer, C., Singh, S., Sourdeval, O., Spickermann, D., Strandgren, J., Tessiot, O., Vercauteren, N., Vial, J., Voigt, A., and Zängl, G.: Large-eddy and storm resolving models for climate prediction - the added value for clouds and precipitation, J. Meteorol. Soc. Japan, 98, doi:10.2151/jmsj. 2020-021, 2020.

Stevens, B., et al.: Atmospheric component of the MPI-M Earth System Model: ECHAM6, J. Adv. Model. Earth Syst. 5: 146–172, doi: 10.1002/jame.20015, 2013.

Stevens, B. and Feingold, G.: Untangling Aerosol Effects on Clouds and Precipitation in a Buffered System, Nature, 461, 607-613, 2009.

Sundqvist, H., et al., Condensation and cloud parameterization studies with a mesoscale numerical weather prediction model, Mon. Weather Rev., 117, 1641–1657, 1989.

Takahashi, T.: High ice crystal production in winter cumuli over the Japan Sea, Geophysical research letters, 20.6, 451-454, 1993.

Takahashi, T., Yoshihiro N., and Yuzuru K.: Possible high ice particle production during graupel–graupel collisions, J. Atmos. Sci., 52.24, 4523-4527, 1995.

Takahashi, T.: Influence of liquid water content and temperature on the form and growth of branched planar snow crystals in a cloud, J. Atmos. Sci., 71.11, 4127-4142, 2014.

Tiedtke, M.: Representation of clouds in large scale models, Mon. Weather Rev., 121, 3040–3061, 1993.

Tompkins, A.: A prognostic parameterization for the subgrid-scale variability of water vapor and clouds in large-scale models and its use to diagnose cloud cover, J. Atmos. Sci., 59:1917- 1942, 2002.

Trömel, S., Quaas, J., Crewell, S., Bott, A., and Simmer, C.: Polarimetric Radar Observations Meet Atmospheric Modelling. 19th International Radar Symposium (IRS), Bonn, doi: 10.23919/IRS.2018.8448121, 2018.

Trömel, S., Ryzhkov, A. V., Hickman, B., Mühlbauer, K., and Simmer, C.: Polarimetric Radar Variables in the Layers of Melting and Dendritic Growth at X Band—Implications for a Nowcasting Strategy in Stratiform Rain, J. Appl. Meteor. Climatol., 58, 2497–2522, doi:10.1175/JAMC-D-19-0056.1, 2019.

Trömel, S., A. V. Ryzhkov, P. Zhang, and C. Simmer: The microphysical information of backscatter differential phase δ in the melting layer, J. Appl. Meteor. Climatol., 53, 2344-2359, 2014.

Verlinde, J., Rambukkange, M. P., Clothiaux, E. E., McFarquhar, G. M., and Eloranta, E. W.: Arctic multilayered, mixed-phase cloud processes revealed in millimeter-wave cloud radar Doppler spectra, J. Geophys. Res. Atmos., 118, 13199 –13213, doi: 10.1002/2013JD020183, 2013.

Vogl, T., Maahn, M., Kneifel, S., Schimmel, W., Moisseev, D., and Kalesse-Los, H.: Using artificial neural networks to predict riming from Doppler cloud radar observations, Atmos. Meas. Tech. Discuss. [preprint], https://doi.org/10.5194/amt-2021-137, in review, 2021.

Voigt, C., Schumann, U., Jurkat, T., Schäuble, D., Schlager, H., Petzold, A., Gayet, J.-F., Krämer, M., Schneider, J., Borrmann, S., Schmale, J., Jessberger, P., Hamburger, T., Lichtenstern, M., Scheibe, M., Gourbeyre, C., Meyer, J., Kübbeler, M., Frey, W., Kalesse, H., Butler, T., Lawrence, M. G., Holzäpfel, F., Arnold, F., Wendisch, M., Döpelheuer, A., Gottschaldt, K., Baumann, R., Zöger, M., Sölch, I., Rautenhaus, M., and Dörnbrack, A.: In-situ observations of young contrails – overview and selected results from the CONCERT campaign, Atmos. Chem. Phys., 10, 9039–9056, doi:10.5194/acp-10-9039-2010, 2010.

Voigt, C., Jeßberger, P., Jurkat, T., Kaufmann, S., Baumann, R., Schlager, H., Bobrowski, N., Guffirda, G., and Salerno, G.: Evolution of CO_2, SO_2, HCl and HNO_3 in the volcanic plumes from Etna, Geophys. Res. Lett., 41, doi:10.1002/2013GL058974, 2014.

Voigt, C., Schumann, U., Minikin, A., Abdelmonem, A., Afchine, A., Borrmann, S., Boettcher, M., Buchholz, B., Bugliaro, L., Costa, A., Curtius, J., Dollner, M., Dörnbrack, A., Dreiling, V., Ebert, V., Ehrlich, A., Fix, A., Forster, L., Frank, F., Fütterer, D., Giez, A., Graf, K., Grooß, J., Groß, S., Heimerl, K., Heinold, B., Hüneke, T., Järvinen, E., Jurkat, T., Kaufmann, S., Kenntner, M., Klingebiel, M., Klimach, T., Kohl, R., Krämer, M., Krisna, T. C., Luebke, A., Mayer, B., Mertes, S., Molleker, S., Petzold, A., Pfeilsticker, K., Port, M., Rapp, M., Reutter, P., Rolf, C., Rose, D., Sauer, D., Schäfler, A., Schlage, R., Schnaiter, M., Schneider, J., Spelten, N., Spichtinger, P., Stock, P., Walser, A., Weigel, R., Weinzierl, B., Wendisch, M., Werner, F., Wernli, H., Wirth, M., Zahn, A., Ziereis, H., and Zöger, M.; ML-CIRRUS: The Airborne Experiment on Natural Cirrus and Contrail Cirrus with the High-Altitude Long-Range Research Aircraft HALO, B. Am. Meteorol. Soc. 98(2), 271-288, doi:bams-d-15-00213.1, 2017.

Voigt, C., Lelieveld, J. , Schlager, H., Schneider, J., Sauer, D., Meerkötter, R., Pöhlker, M., Bugliaro, L., Curtius, J., Erbertseder, T., Hahn, V., Jöckel, P., Li, Q., Marsing, A., Mertens, M., Pöhlker, C., Pöschl, U., Pozzer, A., Tomsche, L., and Schumann, U.: Aerosol and Cloud Changes during the Corona Lockdown in 2020 - First highlights from the BLUESKY campaign; EGU21-13134, https://meetingorganizer.copernicus.org/EGU21/session/40818, 2021.

Wang, M., Zhao, K., Pan, Y., Xue, M.: Evaluation of simulated drop size distributions and microphysical processes using polarimetric radar observations for landfalling Typhoon Matmo (2014), J. Geophys. Res. Atmos., 125, 1-20, doi:10.1029/2019JD031527, 2020.

Weissmann, M., M. Göber, C. Hohenegger, T. Janjic, J. Keller, C. Ohlwein, A. Seifert, S. Trömel, T. Ulbrich, K. Wapler, C. Bollmeyer, H. Deneke: The Hans-Ertel Centre for Weather Research – Research objectives and highlights from its first three years. Meteorol. Z., 23(3), 193 – 208, 2014.

Wendisch, M., Pöschl, U., Andreae, M. O., Machado, L. A. T., Albrecht, R., Schlager, H., Rosenfeld, D., Martin, S. T., Abdelmonem, A., Afchine, A., Araùjo, A. C., Artaxo, P., Aufmhoff, H., Barbosa, H. M. J., Borrmann, S., Braga, R., Buchholz, B., Cecchini, M. A., Costa, A., Curtius, J., Dollner, M., Dorf, M., Dreiling, V., Ebert, V., Ehrlich, A., Ewald, F., Fisch, G., Fix, A., Frank, F., Fütterer, D., Heckl, C., Heidelberg, F., Hüneke, T., Jäkel, E., Järvinen, E., Jurkat, T., Kanter, S., Kästner, U., Kenntner, M., Kesselmeier, J., Klimach, T., Knecht, M., Kohl, R., Kölling, T., Krämer, M., Krüger, M., Krisna, T. C., Lavric, J. V., Longo, K., Mahnke, C., Manzi, A. O., Mayer, B., Mertes, S., Minikin, A., Molleker, S., Münch, S., Nillius, B., Pfeilsticker, K., Pöhlker, C., Roiger, A., Rose, D., Rosenow, D., Sauer, D., Schnaiter, M., Schneider, J., Schulz, C., de Souza, R. A. F., Spanu, A., Stock, P., Vila, D., Voigt, C., Walser, A., Walter, D., Weigel, R., Weinzierl, B., Werner, F., Yamasoe, M. A., Ziereis, H., Zinner, T., and Zöger, M.: ACRIDICON–CHUVA Campaign: Studying Tropical Deep Convective Clouds and Precipitation over Amazonia Using the New German Research Aircraft HALO, B. Am. Meteorol. Soc., 97(10), 1885-1908, doi:bams-d-14-00255.1, 2016.

Wolfensberger, D. and Berne, A.: From model to radar variables: a new forward polarimetric radar operator for COSMO, Atmos. Meas. Tech., 11, 3883-3916, doi: 10.5194/amt-11-3883-2018, 2018.

Xie, X., Evaristo, R., Trömel, S., Saavedra, P., Simmer, C., and Ryzhkov, A.: Radar Observation of Evaporation and Implications for Quantitative Precipitation and Cooling Rate Estimation, J. Atmos. Oceanic Technol. 33(8), 1779-1792, doi:10.1175/JTECH-D-15-0244.1, 2016.

Xie, X., Shrestha, P., Mendrok, J., Carlin, J., Trömel, S., and Blahak, U.: Bonn Polarimetric Radar forward Operator (B-PRO), CRC/TR32 Database (TR32DB), doi:10.5880/TR32DB.41, 2021, (accessed 8 April 2021).

Xue, L., Fan, J., Lebo, Z. J., Wu, W., Morrison, H., Grabowski, W. W., Chu, X., Geresdi, I., North, K., Stenz, R., Gao, Y., Lou, X., Bansemer, A., Heymsfield, A. J., McFarquhar, G. M., and Rasmussen, R. M.: Idealized Simulations of a Squall Line from the MC3E Field Campaign Applying Three Bin Microphysics Schemes: Dynamic and Thermodynamic Structure, Monthly Weather Review, 145(12), 4789-4812, doi:10.1175/MWR-D-16-0385.1, 2017.

You, C.-R., Chung, K.-S., and Tsai, C.-C.: Evaluating the performance of convection-permitting model by using dual-polarimetric radar parameters: Case study of SoWMEX IOP8, Remote Sensing, 12(18):3004, 1-25, doi:10.3390/rs12183004, 2020.

Zängl, G., et al.: The ICON (icosahedral non-hydrostatic) modelling framework of DWD and MPI-M: Description of the non-hydrostatic dynamical core, Q. J. Roy. Meteor. Soc., 141, 563–579, 2015.

Zeng, Y., Janjic, T., Lozar, A. de, Welzbacher, C. A., Blahak, U., and Seifert, A.: Assimilating radar radial wind and reflectivity data in an idealized setup of the COSMO-KENDA system, Atmospheric Research, 249, 105282, doi:10.1016/j.atmosres.2020.105282, 2021a.

Zeng, Y., Janjic, T., Feng, Y., Blahak, U., de Lozar, A., Bauernschubert, E., Stephan, K., and Min, J.: Interpreting estimated observation error statistics of weather radar measurements using the ICON-LAM-KENDA system, Atmos. Meas. Tech., 14, 5735–5756, https://doi.org/10.5194/amt-14-5735-2021, 2021b.

Zeng, Y., Janjic, T., Lozar, A. de, Rasp, S., Blahak, U., Seifert, A., and Craig, G. C.: Comparison of methods accounting for subgrid-scale model error in convective-scale data assimilation, Mon. Wea. Rev., 148, 2457-2477, 2020.

Zeng Y., Janjic, T., Sommer, M., Lozar, A. de, Blahak, U., and Seifert, A.: Representation of model error in convective-scale data assimilation: additive noise based on model truncation error, J. Adv. Model. Earth Sy., 11, 752-770, 2019.

Zeng. Y., Janjic, T., Lozar, A. de, Blahak, U., Reich, H., Keil, C., and Seifert, A.: Representation of model error in convective-scale data assimilation: Additive noise, relaxation methods and combinations, J. Adv. Model. Earth Sy., 10, 2889–2911, 2018.

Zeng, Y., Blahak, U., and Jerger, D.: An efficient modular volume-scanning radar forward operator for NWP models: description and coupling to the COSMO model, Q. J. Roy. Meteor. Soc., 142(701), 3234-3256, 2016

Zhu, K., Xue, M., Ouyang, K., and Jung, Y.: Assimilating polarimetric radar data with an ensemble Kalman filter: OSSEs with a tornadic supercell storm simulated with a two-moment microphysics scheme, Q. J. Roy. Meteor. Soc., 146: 1880– 1900, doi:10.1002/qj.3772, 2020.

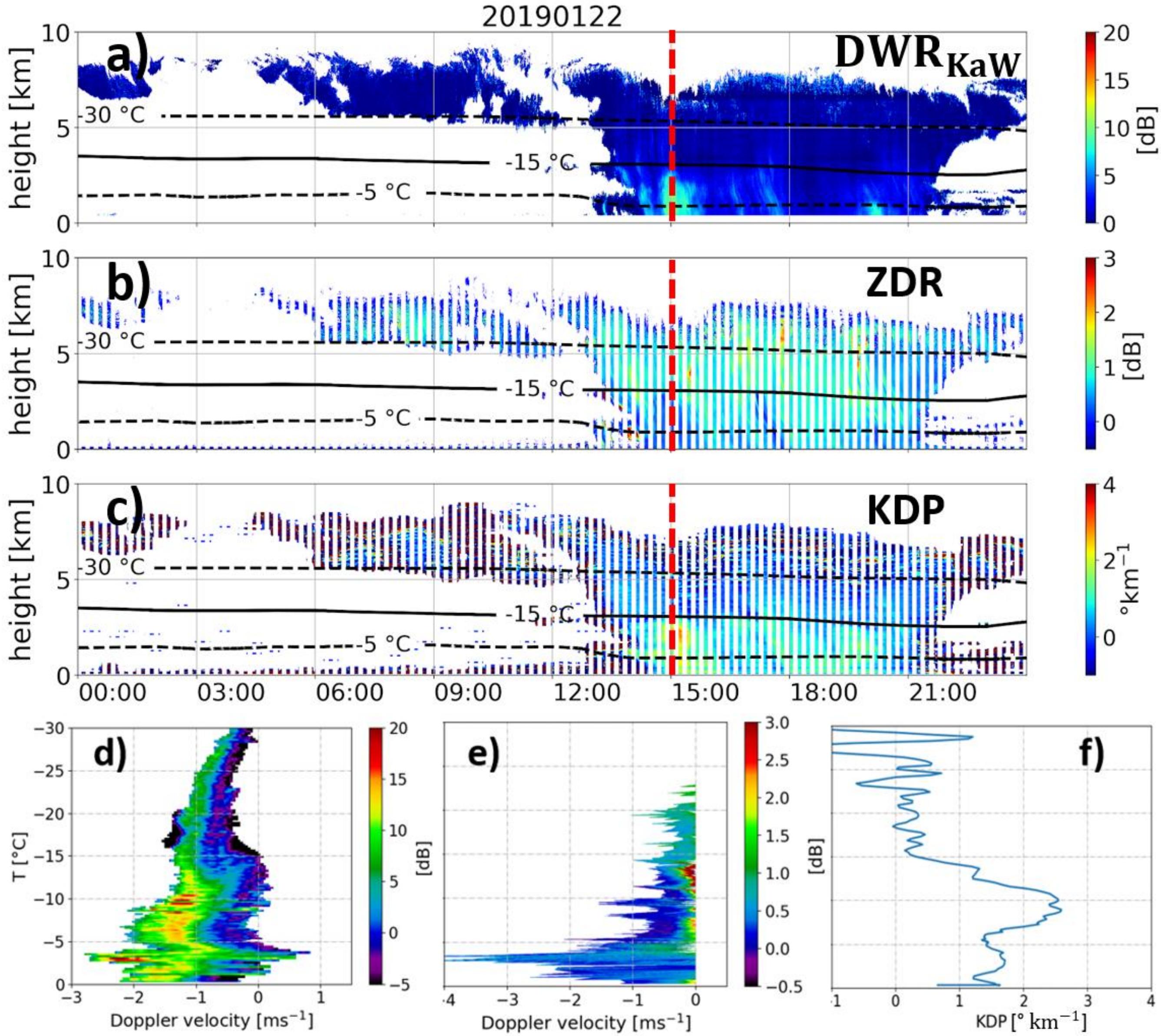

Figure 1: Observations at JOYCE-CF shows a) DWRKaW, b) Z_{DR} (measured at a 30° elevation angle), c) K_{DP} (also measured at 30° elevation angle) on 22 January 2019. Panels d)-f) show the observed DWR-spectrum, Z_{DR}-spectrum and K_{DP}-profile at 15:00 UTC (indicated by the red line in panels a)-c))

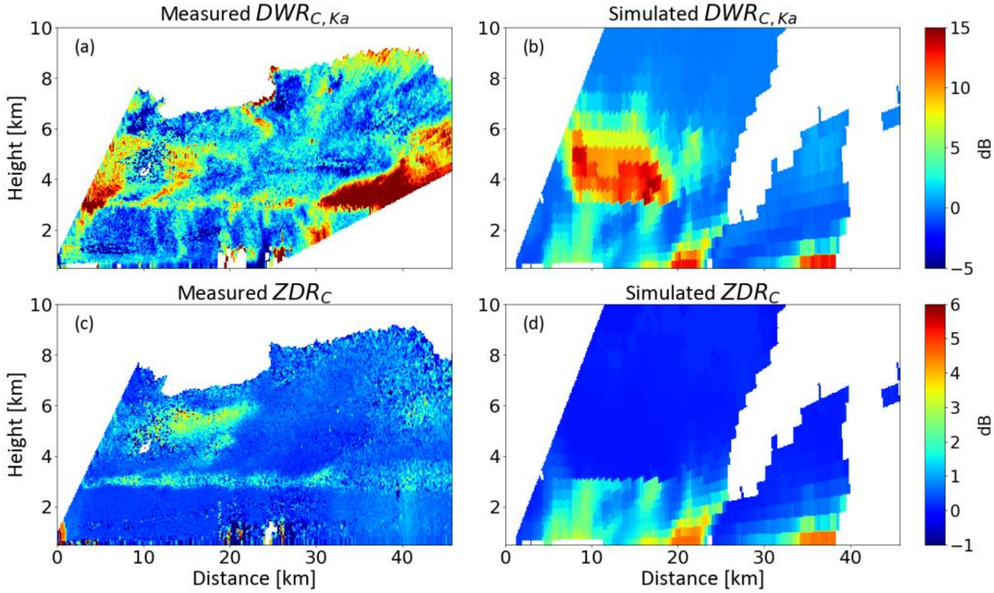

Figure 2 (a) Dual-wavelength ratio between the C-band POLDIRAD and Ka-band miraMACS measurements on the 7th July 2019, (b) simulated dual-wavelength ratio, (c) differential radar reflectivity Z_{DR} measured by the C-band radar POLDIRAD, and (d) simulated Z_{DR} of a comparable, but not identical, precipitation event using the P3 scheme (Morrison and Milbrandt, 2015).

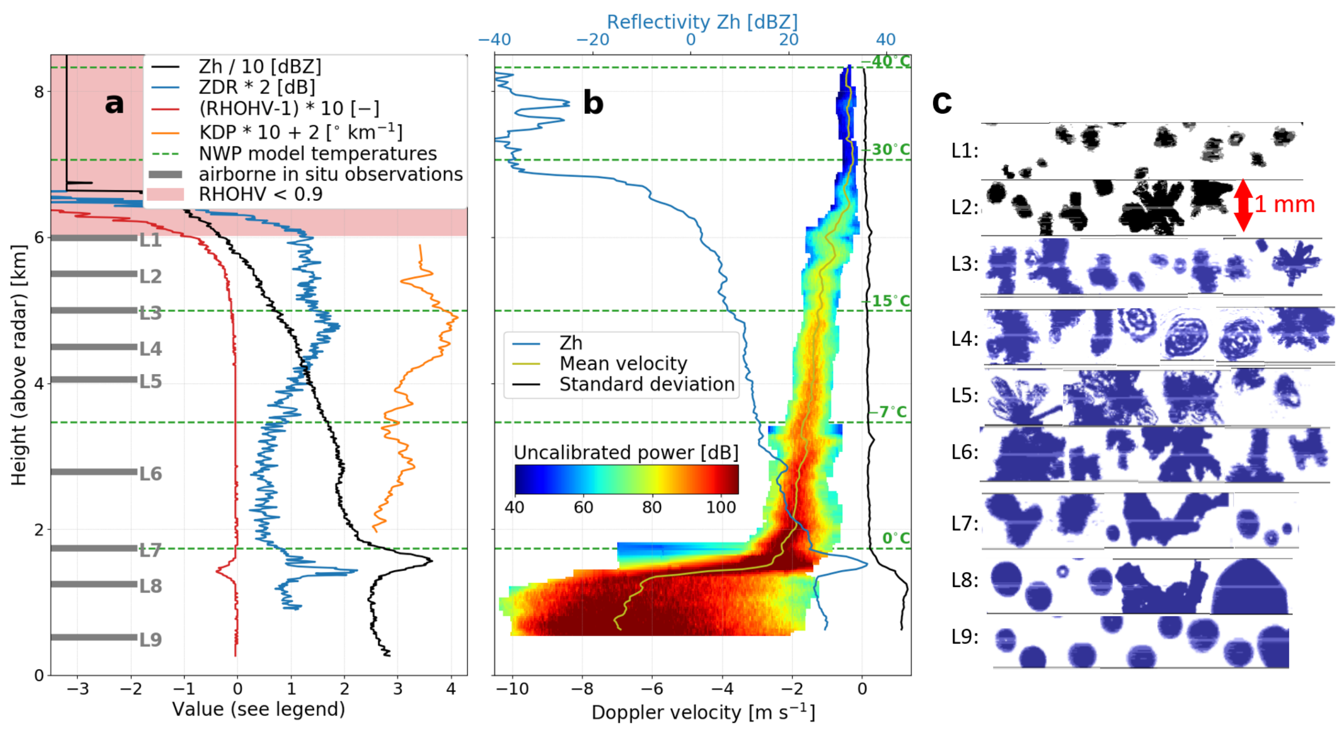

Figure 3: Measurements of slant-viewing and zenith-pointing polarimetric C-band weather radar scans with NWP model based temperature levels and airborne in-situ observations: (a) quasi-vertical profiles (QVPs) of radar reflectivity Z_H, differential reflectivity Z_{DR}, copolar cross-channel correlation coefficient ρ_{HV}, and the specific differential phase K_{DP} estimated from (noisy) measurements of the differential phase by aggressive filtering above the melting layer; (b) average Doppler spectra from a 15 s birdbath scan and corresponding first 3 moments at each radar bin height: reflectivity, power-weighted mean velocity and standard deviation; (c) in situ particle images (downward-looking projection images) collected at altitudes L1 to L9.

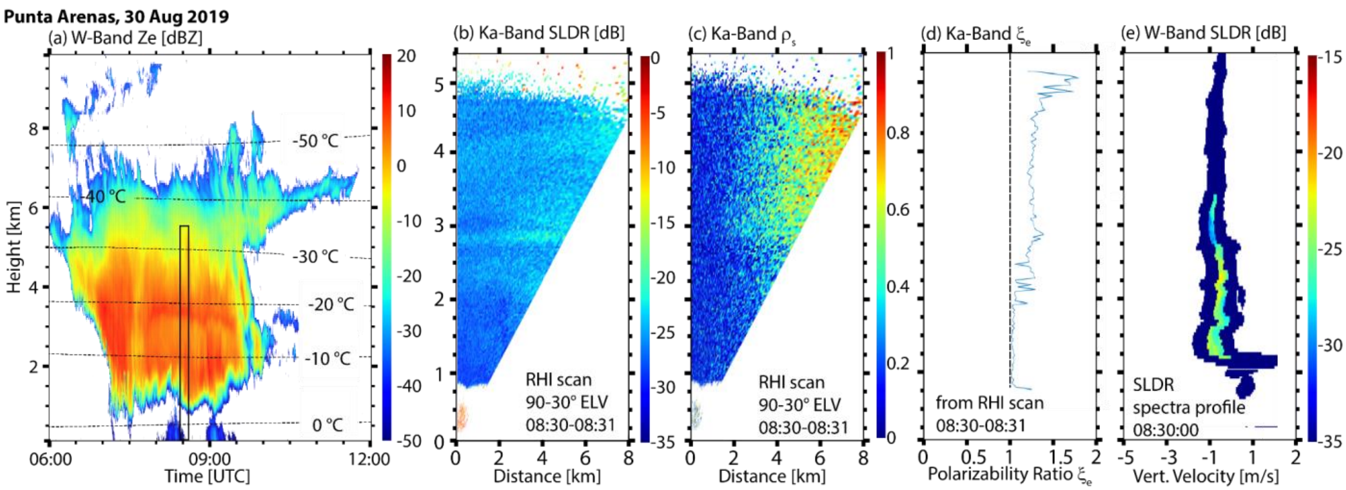

Figure 4: Case study of a deep mixed-phase cloud event observed with multiwavelength polarimetric cloud radars at Punta Arenas, Chile, on 30 August 2019. (a) vertical-pointing W-Band (94-GHz) radar reflectivity factor Ze and isolines of modeled air temperature, (b) and (c) Ka-Band (35-GHz) RHI scans (90°-30° elevation) of slanted linear depolarization ratio SLDR and co-cross correlation coefficient in the slanted basis ρ_s, respectively, from 08:30-08:31 UTC, (d) profile of the shape index polarizability ratio (ξ_e) obtained from the RHI scans shown in (b) and (c), and (e) height spectrogram (at 90° elevation) of W-Band SLDR from 08:30:00 UTC. The time and height frame of panels (b-e) is indicated by the black rectangle in (a).

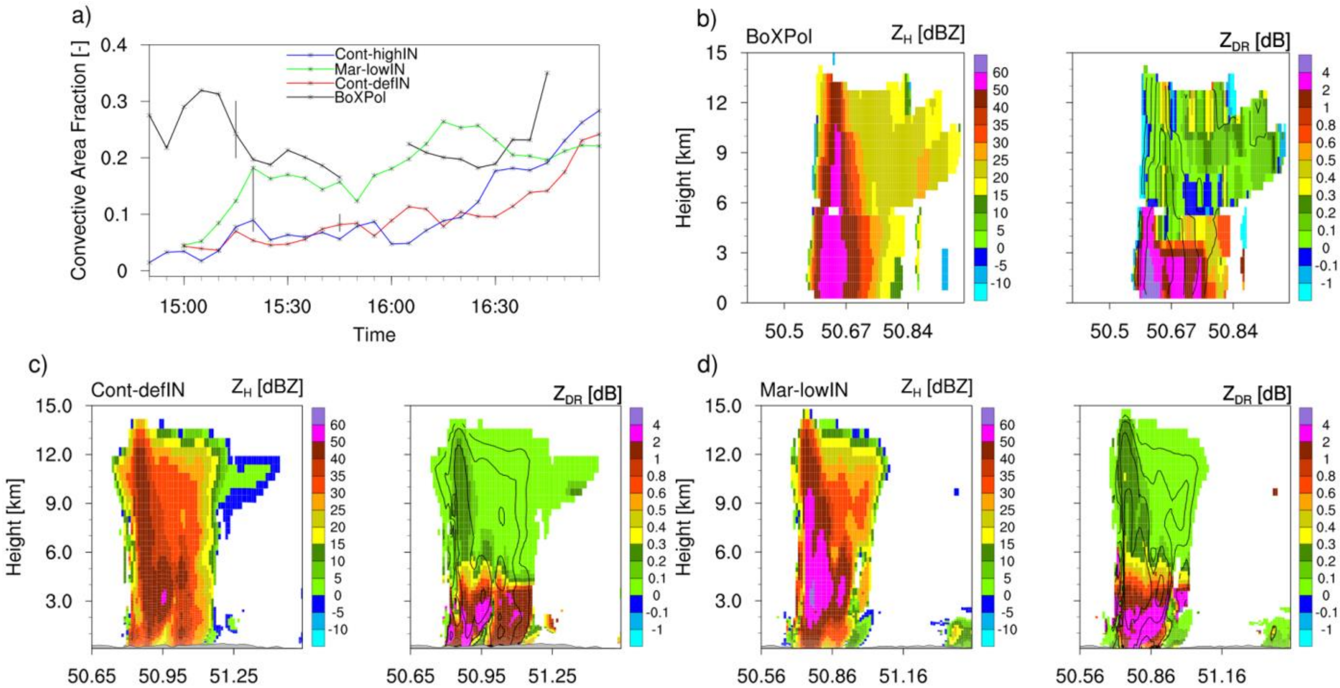

Figure 5: Time-series of Convective Area Fraction (CAF) evolution (panel a) and reconstructed observed (panel b) and simulated/synthetic range-height-indicators (RHI) of horizontal reflectivity Z_H and differential reflectivity Z_{DR} (panels c and d). Synthetic RHIs are based on simulations for actual land-cover with different perturbations of CN and IN concentrations, where Cont-defIN indicates continental aerosol with default IN concentration and Mar-lowIN indicates maritime aerosol with low IN concentration. The gaps in the BoXPol-observed CAF time series are due to strong attenuation. The vertical grey bars (panel a) indicate the times at which the RHIs are compared.

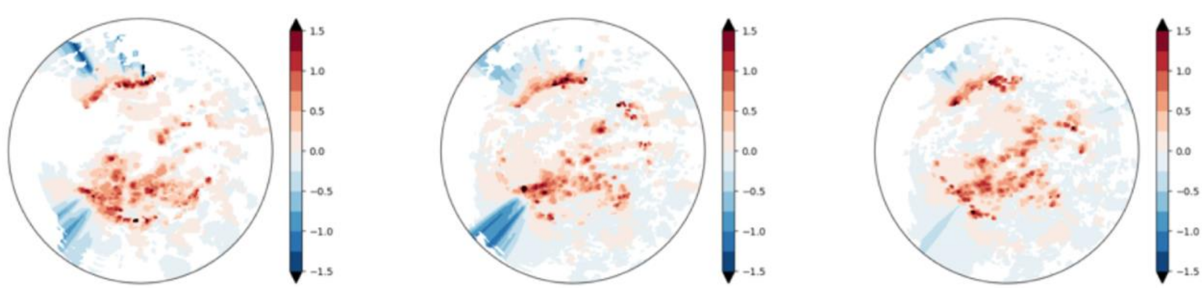

Figure 6: Synthetic PPI of Z_{DR} at 0.5 deg elevation for the DWD radar site Neuheilenbach based on the analysis obtained for June 4 at 16:00 UTC by assimilation of radar reflectivity and using three different ways to specify the model error: large scale uncertainty (left), large plus unresolved scales uncertainty (middle) and in addition the use of the warm bubble approach (right).

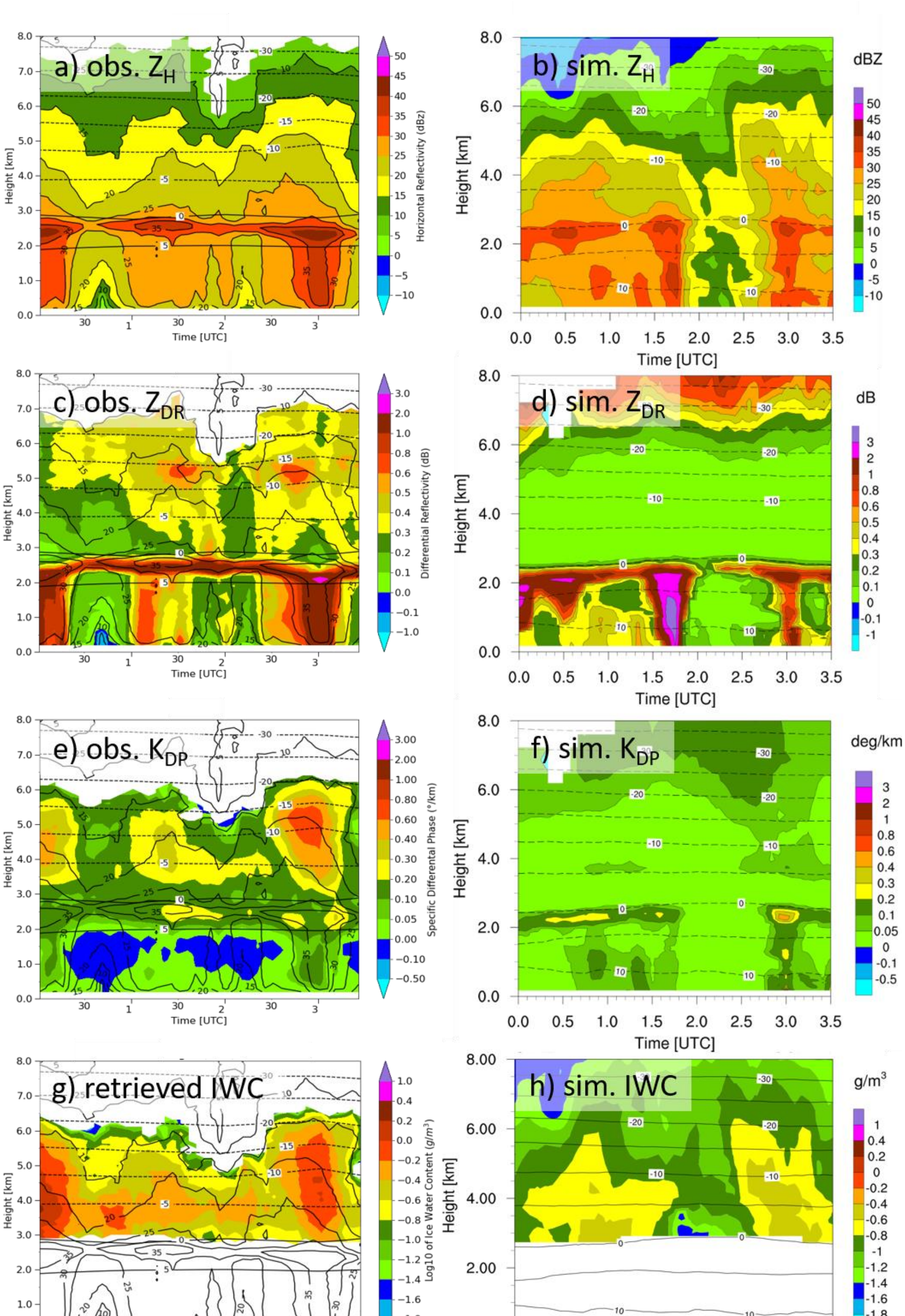

Figure 7: Quasi-vertical profiles (QVPs) of observed (left column) and simulated (right column) polarimetric radar variables horizontal reflectivity Z_H (panels a and b), differential reflectivity Z_{DR} (panels c and d), specific differential phase K_{DP} (panels e and f), together with radar-retrieved (panel g) and simulated ice water content (IWC, panel h). The QVPs show a stratiform rain event

observed on 7 October 2014 between 0:00 and 3:30 UTC with the polarimetric X-band radar in Bonn, BoXPol, and simulated with COSMO version 5.1 and the 2-moment cloud microphysics scheme.

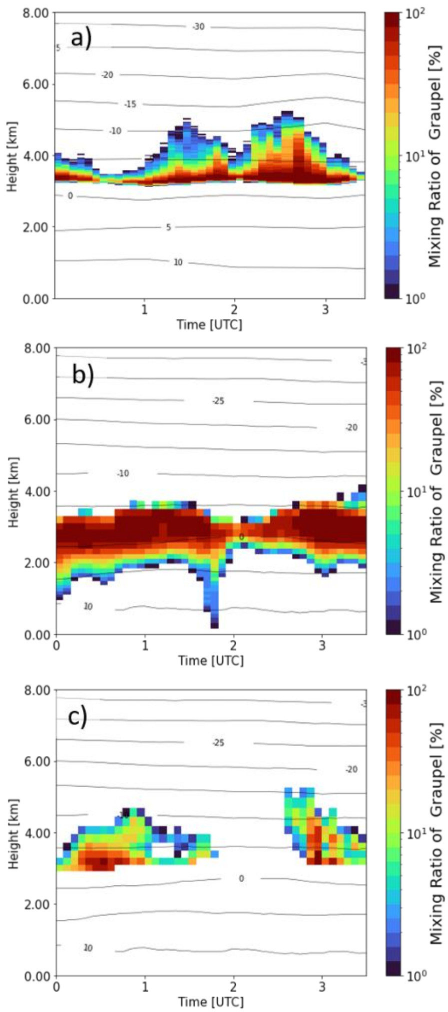

Figure 8: Retrieved and simulated graupel mixing ratios, defined as the percentage of graupel in the total hydrometeor mass, for the stratiform rain event shown in Fig. 7 (7 October 2014, 0:00-3:30 UTC). An advanced hydrometeor classification and quantification algorithm has been applied to polarimetric BoXPol measurement (panel a) and to simulated radar variables based on COSMO simulations (panel c) and compared to the COSMO-simulated graupel mixing (panel b).

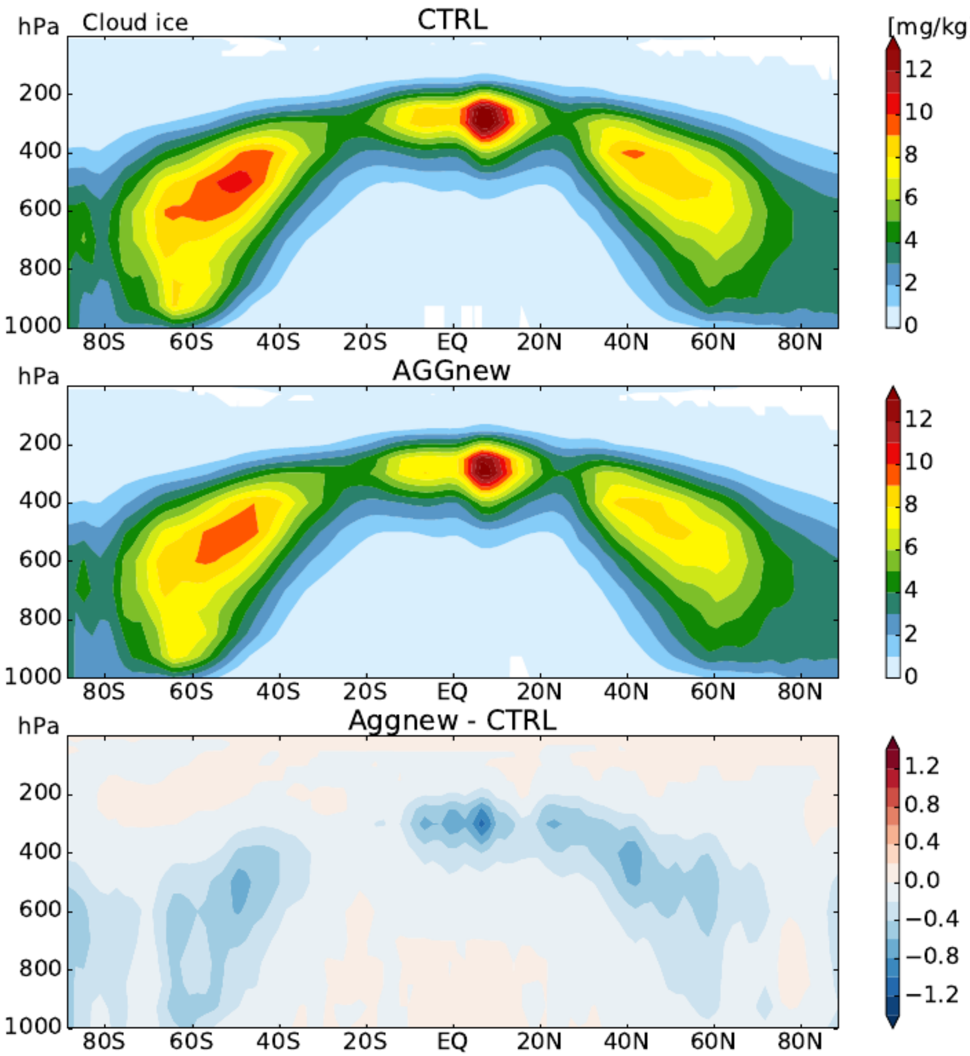

Figure 9: Specific ice water, q_i, [g kg^{-1}] as zonal, annual mean for (top) standard ICON GCM output, (middle) aggregation parameterization revised as stochastic parameterization drawing from the q_i subgrid-variability PDF, and (bottom) difference between the two.